study indicate that apoptosis occurs in kidneys after I/R, and this may therefore be an important phenomenon in clinical renal transplantation. Although the overexpression of Bcl-2 is not yet practicable in clinical settings, the augmentation of Bcl-2 in transplanted kidneys may be of therapeutic relevance for either minimizing or abolishing apoptotic cell death, thereby improving the outcome after kidney transplantation.

REFERENCES

1. Beeri, R.; Symon, Z.; Brezis, M.; Ben-Sasson, S. A.; Baehr, P. H.; Rosen, S.; Zager, R. A. Rapid DNA fragmentation from hypoxia along the thick ascending limb of rat kidneys. Kidney Int. 47(6):1806–1810; 1995.
2. Border, W. A.; Noble, N. A. TGF-beta in kidney fibrosis: A target for gene therapy. Kidney Int. 51(5):1388–1396; 1997.
3. Daemen, M. A.; van de Ven, M. W.; Heineman, E.; Buurman, W. A. Involvement of endogenous interleukin-10 and tumor necrosis factor-alpha in renal ischemia-reperfusion injury. Transplantation 67(6):792–800; 1999.
4. Foyouzi-Youssefi, R.; Arnaudeau, S.; Borner, C.; Kelley, W. L.; Tschopp, J.; Lew, D. P.; Demaurex, N.; Krause, K. H. Bcl-2 decreases the free Ca2+ concentration within the endoplasmic reticulum. Proc. Natl. Acad. Sci. USA 97(11):5723–5728; 2000.
5. Friedrichs, G. S.; Kilgore, K. S.; Manley, P. J.; Gralinski, M. R.; Lucchesi, B. R. Effects of heparin and N-acetyl heparin on ischemia/reperfusion-induced alterations in myocardial function in the rabbit isolated heart. Circ. Res. 75(4):701–710; 1994.
6. Gobe, G.; Zhang, X. J.; Willgoss, D. A.; Schoch, E.; Hogg, N. A.; Endre, Z. H. Relationship between expression of Bcl-2 genes and growth factors in ischemic acute renal failure in the rat. J. Am. Soc. Nephrol. 11(3):454–467; 2000.
7. Gulati, S.; Singh, A. K.; Irazu, C.; Orak, J.; Rajagopalan, P. R.; Fitts, C. T.; Singh, I. Ischemia-reperfusion injury: Biochemical alterations in peroxisomes of rat kidney. Arch. Biochem. Biophys. 295(1):90–100; 1992.
8. Hauet, T.; Goujon, J. M.; Vandewalle, A. To what extent can limiting cold ischaemia/reperfusion injury prevent delayed graft function? Nephrol. Dial. Transplant. 16(10): 1982–1985; 2001.
9. Kaminski, K. A.; Bonda, T. A.; Korecki, J.; Musial, W. J. Oxidative stress and neutrophil activation—the two keystones of ischemia/reperfusion injury. Int. J. Cardiol. 86(1):41–59; 2002.
10. Korsmeyer, S. J.; Shutter, J. R.; Veis, D. J.; Merry, D. E.; Oltvai, Z. N. Bcl-2/Bax: A rheostat that regulates an antioxidant pathway and cell death. Semin. Cancer Biol. 4(6): 327–332; 1993.
11. Kroemer, G. The proto-oncogene Bcl-2 and its role in regulating apoptosis. Nat. Med. 3(6):614–620; 1997.
12. Lacronique, V.; Mignon, A.; Fabre, M.; Viollet, B.; Rouquet, N.; Molina, T.; Porteu, A.; Henrion, A.; Bouscary, D.; Varlet, P.; Joulin, V.; Kahn, A. Bcl-2 protects from lethal hepatic apoptosis induced by an anti-Fas antibody in mice. Nat. Med. 2(1):80–86; 1996.
13. Lieberthal, W.; Menza, S. A.; Levine, J. S. Graded ATP depletion can cause necrosis or apoptosis of cultured mouse proximal tubular cells. Am. J. Physiol. 274(2 Pt. 2):F315–327; 1998.
14. Maulik, N.; Sasaki, H.; Galang, N. Differential regulation of apoptosis by ischemia-reperfusion and ischemic adaptation. Ann. NY Acad. Sci. 874:401–411; 1999.
15. Menger, M. D.; Pelikan, S.; Steiner, D.; Messmer, K. Microvascular ischemia-reperfusion injury in striated muscle: Significance of "reflow paradox". Am. J. Physiol. 263(6 Pt. 2):H1901–1906; 1992.
16. Nogae, S.; Miyazaki, M.; Kobayashi, N.; Saito, T.; Abe, K.; Saito, H.; Nakane, P. K.; Nakanishi, Y.; Koji, T. Induction of apoptosis in ischemia-reperfusion model of mouse kidney: Possible involvement of Fas. J. Am. Soc. Nephrol. 9(4):620–631; 1998.
17. Rhyu, D. Y.; Yang, Y.; Ha, H.; Lee, G. T.; Song, J. S.; Uh, S. T.; Lee, H. B. Role of reactive oxygen species in TGF-beta1-induced mitogen-activated protein kinase activation and epithelial-mesenchymal transition in renal tubular epithelial cells. J. Am. Soc. Nephrol. 16(3):667–675; 2005.
18. Terasaki, P. I.; Koyama, H.; Cecka, J. M.; Gjertson, D. W. The hyperfiltration hypothesis in human renal transplantation. Transplantation 57(10):1450–1454; 1994.
19. Tilney, N. L.; Guttmann, R. D. Effects of initial ischemia/reperfusion injury on the transplanted kidney. Transplantation 64(7):945–947; 1997.
20. Tsujimoto, Y.; Nakagawa, T.; Shimizu, S. Mitochondrial membrane permeability transition and cell death. Biochim. Biophys. Acta 1757(9–10):1297–1300; 2006.
21. Tsujimoto, Y.; Shimizu, S. Bcl-2 family: life-or-death switch. FEBS Lett. 466(1):6–10; 2000.
22. Tsujimoto, Y.; Shimizu, S. Role of the mitochondrial membrane permeability transition in cell death. Apoptosis 12(5):835–840; 2007.
23. Tullius, S. G.; Tilney, N. L. Both alloantigen-dependent and -independent factors influence chronic allograft rejection. Transplantation 59(3):313–318; 1995.
24. Yamabe, K.; Shimizu, S.; Kamiike, W.; Waguri, S.; Eguchi, Y.; Hasegawa, J.; Okuno, S.; Yoshioka, Y.; Ito, T.; Sawa, Y.; Uchiyama, Y.; Tsujimoto, Y.; Matsuda, H. Prevention of hypoxic liver cell necrosis by in vivo human bcl-2 gene transfection. Biochem. Biophys. Res. Commun. 243(1):217–223; 1998.
25. Zhou, W.; Farrar, C. A.; Abe, K.; Pratt, J. R.; Marsh, J. E.; Wang, Y.; Stahl, G. L.; Sacks, S. H. Predominant role for C5b-9 in renal ischemia/reperfusion injury. J. Clin. Invest. 105(10):1363–1371; 2000.
26. Zoratti, M.; Szabo, I. The mitochondrial permeability transition. Biochim. Biophys. Acta 1241(2):139–176; 1995.

Lysophosphatidylcholine as a death effector in the lipoapoptosis of hepatocytes[S]

Myoung Sook Han,[1,*] Sun Young Park,[1,*] Koei Shinzawa,[†] Sunshin Kim,[*] Kun Wook Chung,[*] Ji-Hyun Lee,[§] Choon Hyuck Kwon,[**] Kwang-Woong Lee,[**] Joon-Hyoek Lee,[*] Cheol Keun Park,[††] Woo Jin Chung,[§§] Jae Seok Hwang,[§§] Ji-Jing Yan,[***] Dong-Keun Song,[***] Yoshihide Tsujimoto,[†] and Myung-Shik Lee[2,*]

Departments of Medicine,* Surgery,** and Pathology,†† Samsung Medical Center, Sungkyunkwan University School of Medicine, Seoul 135-710, Korea; Laboratory of Molecular Genetics,† Department of Medical Genetics, Osaka University Medical School and Solution Oriented Research for Science and Technology (SORST) of the Japan Science and Technology Corporation, Osaka 565-1871, Japan; Samsung Biomedical Research Institute,§ Seoul 135-710, Korea; Department of Medicine,§§ Keimyung University School of Medicine, Daegu 700-712, Korea; and Department of Pharmacology,*** College of Medicine, Hallym University, Chunchon, Gangwon 200-702, Korea

Abstract The pathogenesis of nonalcoholic steatohepatitis (NASH) is unclear, despite epidemiological data implicating FFAs. We studied the pathogenesis of NASH using lipoapoptosis models. Palmitic acid (PA) induced classical apoptosis of hepatocytes. PA-induced lipoapoptosis was inhibited by acyl-CoA synthetase inhibitor but not by ceramide synthesis inhibitors, suggesting that conversion products other than ceramide are involved. Phospholipase A_2 (PLA_2) inhibitors blocked PA-induced hepatocyte death, suggesting an important role for PLA_2 and its product lysophosphatidylcholine (LPC). Small interfering RNA for Ca^{2+}-independent phospholipase A_2 ($iPLA_2$) inhibited the lipoapoptosis of hepatocytes. PA increased LPC content, which was reversed by $iPLA_2$ inhibitors. Pertussis toxin or dominant-negative $G\alpha_i$ mutant inhibited hepatocyte death by PA or LPC acting through G-protein-coupled receptor (GPCR)/$G\alpha_i$. PA decreased cardiolipin content and induced mitochondrial potential loss and cytochrome *c* translocation. Oleic acid inhibited PA-induced hepatocyte death by diverting PA to triglyceride and decreasing LPC content, suggesting that FFAs lead to steatosis or lipoapoptosis according to the abundance of saturated/unsaturated FFAs. LPC administration induced hepatitis in vivo. LPC content was increased in the liver specimens from NASH patients. These results demonstrate that LPC is a death effector in the lipoapoptosis of hepatocytes and suggest potential therapeutic values of PLA_2 inhibitors or GPCR/$G\alpha_i$ inhibitors in NASH.—Han, M. S., S. Y. Park, K. Shinzawa, S. Kim, K. W. Chung, J-H. Lee, C. H. Kwon, K-W. Lee, J-H. Lee, C. K. Park, W. J. Chung, J. S. Hwang, J-J. Yan, D-K. Song, Y. Tsujimoto, and M-S. Lee. Lysophosphatidylcholine as a death effector in the lipoapoptosis of hepatocytes. *J. Lipid Res.* 2008. 49: 84–97.

Supplementary key words fatty acids • phospholipase A_2 • steatohepatitis • triglyceride • ceramide

Nonalcoholic fatty liver disease (NAFLD) is characterized by lipid deposition in hepatocytes without alcohol abuse (1). Nonalcoholic steatohepatitis (NASH) is a severe form of NAFLD accompanied by necrosis, inflammation, and fibrosis (2). Although steatosis alone is nonprogressive, 20% of NASH progresses to cirrhosis (1). The pathogenesis of NAFLD is not clearly understood and may entail multiple injuries from increased FFAs, oxidative stress, lipid peroxidation, and tumor necrosis factor-α (1, 3).

NAFLD is frequently associated with type 2 diabetes, obesity, and insulin resistance, which constitute important components of the metabolic syndrome (2). FFAs released

Abbreviations: A_{630}, absorption at 630 nm; ALT, alanine aminotransferase; AST, aspartate aminotransferase; BEL, bromoenol lactone; $cPLA_2$, cytoplasmic phospholipase A_2; DAG, diacylglycerol; GPCR, G-protein-coupled receptor; $iPLA_2$, Ca^{2+}-independent phospholipase A_2; JNK, c-Jun *N*-terminal kinase; LPA, lysophosphatidic acid; LPC, lysophosphatidylcholine; LPE, lysophosphatidylethanolamine; LPG, lysophosphatidylglycerol; LPI, lysophosphatidylinositol; LPS, lysophosphatidylserine; MAFP, methyl arachidonyl fluorophosphonate; MTT, 3-[4,5-dimethylthiazol-2-yl]-2,5-diphenyltetrazolium bromide; NAFLD, nonalcoholic fatty liver disease; NAO, 10-*N*-nonyl acridine orange; NASH, nonalcoholic steatohepatitis; OA, oleic acid; PA, palmitic acid; $PACOCF_3$, palmitoyl trifluoromethyl ketone; PC, phosphatidylcholine; PI, propidium iodide; PKC, protein kinase C; PLA_2, phospholipase A_2; PTX, pertussis toxin; siRNA, small interfering RNA; TG, triglyceride; TUNEL, terminal deoxynucleotidyl transferase mediated dUTP nick end labeling.

[1] M. S. Han and S. Y. Park contributed equally to this work.

[2] To whom correspondence should be addressed.
e-mail: mslee@smc.samsung.co.kr

[S] The online version of this article (available at http://www.jlr.org) contains supplementary data in the form of three figures.

Manuscript received 16 April 2007 and in revised form 14 September 2007 and in re-revised form 17 October 2007.

Published, JLR Papers in Press, October 18, 2007.
DOI 10.1194/jlr.M700184-JLR200

from visceral fat of obese subjects are strong culprits in insulin resistance. Recent papers have suggested a potential role for FFAs in insulin deficiency as well as in insulin resistance, consistent with FFA-mediated injury of pancreatic β-cells and several other tissues (4).

FFAs may be related to NAFLD through their increased flux from visceral fat to the liver. Because of strong epidemiological and in vivo data suggesting the relationship between FFAs and NAFLD, several in vitro experiments studying hepatocyte injury by FFAs have been conducted, which suggested possible roles for the mitochondrial pathway, lysosomal pathway, endoplasmic reticulum stress, and c-Jun N-terminal kinase (JNK) activation in the lipoapoptosis of hepatocytes (5–9). However, the intracellular metabolites of FFAs that are directly responsible for such intracellular events are not clearly identified. We found evidence supporting the role of lysophosphatidylcholine (LPC) produced by phospholipase A_2 (PLA_2), which catalyzes the hydrolysis of the fatty acyl ester bond at the *sn*-2 position of glycerophospholipids and has been implicated in several types of cell death (10–13), as an effector in the lipoapoptosis of hepatocytes (Fig. 1).

MATERIALS AND METHODS

Reagents

Palmitoyl trifluoromethyl ketone ($PACOCF_3$) and methyl arachidonyl fluorophosphonate (MAFP) were from Calbiochem. zVAD-fmk was from Enzyme Systems (Livermore). All other chemicals were obtained from Sigma unless stated otherwise.

Cell death assay

Chang cells grown in DMEM-10% FBS were treated with FFAs or other reagents for 24 h unless stated otherwise. We chose a 24 h treatment protocol because our time course study revealed that cell death >50% with full-blown features of apoptosis, such as nuclear condensation/fragmentation and sub-G1 DNA peak, occurred at 24 h after treatment. Palmitic acid (PA) solution was made according to a previously published protocol with modifications (14). Briefly, PA stock solution (50 mM) was prepared by dissolving in 70% ethanol and heating at 50°C. Working PA solution was made by diluting stock solution in 2% fatty acid-free BSA-DMEM-10% FBS, because the concentration of FFAs, particularly that of PA, is quite low in 10% FBS, whereas cells were healthier with serum for prolonged experiments. 3-[4,5-Dimethylthiazol-2-yl]-2,5-diphenyltetrazolium bromide (MTT) assay, Hoechst 33258/propidium iodide (PI) staining, and DNA ploidy analysis were conducted as described (15). We used the MTT assay throughout the study because the results from the MTT assay were consistent with those of other cell death assays such as Hoechst/PI staining or DNA ploidy analysis in our pilot study. In some experiments, cells were pretreated with inhibitors for 1 h before PA treatment. To assess the death of primary murine hepatocytes, a lactate dehydrogenase release assay was used (12). Percentage cell death was calculated as (experimental release − spontaneous release)/(total release − spontaneous release) × 100.

Ammonia removal

Ammonia concentration in the culture supernatant was measured using a commercial kit (Asan Pharmaceuticals). Briefly, cells were incubated in a medium containing test reagents and 2 mM NH_4Cl for 48 h. The absorption at 630 nm (A_{630}) by indophenol generated from ammonia was measured. Percentage removal was calculated as [1 − (A_{630} with added ammonia to the

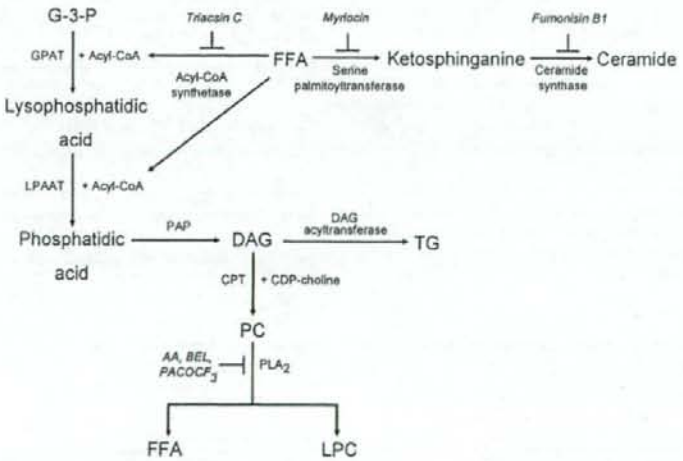

Fig. 1. Metabolism of FFAs. FFAs may be incorporated into ceramide, which could be an important death effector, or into diacylglycerol (DAG), which could be converted to lysophosphatidylcholine (LPC) or triglyceride (TG). AA, aristolochic acid; BEL, bromoenol lactone; CPT, CDP-choline:1,2-DAG phosphocholine transferase; G-3-P, glycerol-3-phosphate; GPAT, glycerophosphate acyltransferase; LPAAT, lysophosphatidic acid acyltransferase; PAP, phosphatidic acid phosphohydrolase; PC, phosphatidylcholine; $PACOCF_3$, palmitoyl trifluoromethyl ketone; PLA_2, phospholipase A_2.

cells − basal A_{630} of the cells)/(A_{630} with added ammonia to the blank − basal A_{630} of the blank)].

Small interfering RNA and RT-PCR

Small interfering RNAs (siRNAs) for human Ca^{2+}-independent phospholipase A_2 β (iPLA$_2$β) (AAT TGC GCG GAG AAC GAG GAG), iPLA$_2$γ (AAA ATG AAC ATT TCC GGG ACA), and an irrelevant siRNA purchased from Invitrogen were transfected using Oligofectamine (Invitrogen) according to the manufacturer's protocol. Expression of iPLA$_2$β and iPLA$_2$γ at the RNA level was determined by RT-PCR using specific primer sets. Expression of markers for hepatocytes was also tested by RT-PCR using specific primer sets (16).

Measurement of LPC

Intracellular LPC content was measured using an enzymatic assay reported previously (17). Briefly, sample was added to the mixture of 100 mM Tris-HCl, pH 8.0, 0.01% Triton X-100, 1 mM $CaCl_2$, 3 mM *N*-ethyl-*N*-[2-hydroxy-3-sulfopropyl]3-methylaniline, 10 U/ml peroxidase, 0.1 U/ml glycerophosphorylcholine phosphodiesterase, and 10 U/ml choline oxidase. After incubation at 37°C for 5 min, reagent mixture containing 100 mM Tris-HCl, pH 8.0, 5 mM 4-aminoantipyrine, 0.01% Triton X-100, and 20 U/ml lysophospholipase was added. After incubation for another 5 min, A_{570} was measured using LPC 16:0 as a standard.

Transfection

Chang cells stably expressing a dominant-negative Gα$_{i2}$ mutant (α$_{i2}$G203T) (18) or wild-type Gα$_{i2}$ (University of Missouri-Rolla cDNA Resource Center) were produced by transfection with FuGENE 6 (Roche) and selection with G418 for 3 weeks.

Mitochondrial events

After incubating cells with 0.4 μM 10-*N*-nonyl acridine orange (NAO; Molecular Probes) at 37°C, NAO fluorescence was measured by flow cytometry (19). Mitochondrial potential was measured by calculating A_{590}/A_{530} after incubating cells with 10 μg/ml JC-1 (Molecular Probes) for 10 min (20).

Cell fractionation

Cells lysed in an isotonic buffer were fractionated as described (20). The heavy membrane fraction and cytosolic fraction were subjected to Western blotting using specific antibodies against cytochrome *c* (PharMingen) or Bid (Santa Cruz) (15). The purity of the heavy membrane and cytosolic fractions was confirmed by Western blotting using anti-Cox4 and anti-IκB antibody, respectively. Expression of phosphorylated JNK and total JNK in the whole cell lysate was studied by Western blotting using specific antibodies (Cell Signaling).

Oil Red O staining

Cells were fixed with 10% formaldehyde for 1 h. After staining with 3 μg/ml Oil Red O solution for 15 min, dye was extracted by isopropanol and A_{540} was measured.

Human liver biopsy

Human liver tissue was obtained from the nontumor part of the livers from patients undergoing hepatic resection for metastatic colon cancer at Samsung Medical Center. The absence of cancer and cirrhosis was confirmed grossly and microscopically. The isolation of hepatocytes was performed using a two-step collagenase perfusion technique as described previously (21). After isolation, primary hepatocytes were cultured in a modified hormonally defined medium (William's E medium supplemented with 20 μg/l epidermal growth factor, 10 mg/l insulin, 1.7 mg/l hydrocortisone, 24.97 μg/l $CuSO_4 \cdot 5H_2O$, 14.38 pg/l $ZnSO_4 \cdot 7H_2O$, 3 μg/l H_2SeO_3, 50 mg/l linoleic acid, 1.05 g/l $NaHCO_3$, and 1.19 g/l HEPES) (22). Aspartate aminotransferase/alanine aminotransferase (AST/ALT) levels were measured using the FPC 3000 Blood Chemistry Analyzer (Fuji). Ultrasonography-guided liver biopsy was conducted in patients with clinical findings compatible with NAFLD without history of alcoholism (alcohol consumption < 140 g/week) using 18-gauge Solco needles inserted through the intercostal space. All patients had serum AST/ALT levels > 60 U/l and body mass index > 25 without recent history of diet control or parenteral nutrition. All were negative for viral markers, autoantibodies related to liver diseases, clinical evidence of cirrhosis, lipodystrophy, or Wilson's disease, and were not taking drugs related to lipid metabolism. Informed consent was obtained from all participants. All human studies were approved by the Institutional Review Board of Samsung Medical Center. An experienced hepatopathologist blinded to subject details scored the liver biopsy specimens according to a published classification (2).

Terminal deoxynucleotidyl transferase mediated dUTP nick end labeling staining

Terminal deoxynucleotidyl transferase mediated dUTP nick end labeling (TUNEL) staining of mouse liver tissues was conducted as described (15). Briefly, formalin-fixed sections were deparaffinized and microwaved in 0.01 M sodium citrate buffer (pH 6.0) and 0.1% Triton X-100. They were incubated with TUNEL reagents (Roche Molecular Biochemicals) at 37°C for 60 min. After washing, they were further incubated with Convert-POD for 30 min. Diaminobenzidine was used as a color substrate.

Mouse hepatocytes

Primary murine hepatocytes were isolated from C57BL/6 mice using the retrograde two-step collagenase perfusion technique (23). LPC (kindly provided by K-S. Song, Doosan Pharmaceutical; purity > 99%) dissolved in PBS-2% BSA by sonication was injected into the tail vein of ICR mice. All animal experiments were conducted in accordance with the institutional guidelines of the Osaka University Animal Facility and the Samsung Medical Center Animal Facility.

Measurement of iPLA$_2$ activity

Activity of iPLA$_2$ was measured using a commercial kit (Cayman) with modifications (24). Briefly, cells were collected with a cell scraper, sonicated, and centrifuged at 20,000 *g* at 4°C for 20 min. The supernatant was removed, and the concentration of proteins was determined. iPLA$_2$ activity was assayed by incubating the samples with arachidonoyl thio-PC for 1 h at 25°C in a Ca^{2+}-free buffer (300 mM NaCl, 0.5% Triton X-100, 60% glycerol, 4 mM EGTA, 10 mM HEPES, pH 7.4, and 2 mg/ml BSA). The reaction was terminated by adding 5,5′-dithio-bis-2-nitrobenzoic acid for 5 min, and A_{405} was measured. The specific activity of iPLA$_2$ was calculated and expressed as absorbance per milligram of protein. The background activity was subtracted from all readings.

Statistical analysis

All values are expressed as means ± SD from more than three independent experiments performed in triplicate. Two-tailed Student's *t*-test was used to compare values between two groups. ANOVA was used for multiple comparisons. The Scheffé test was used to compare two groups once ANOVA showed significant differences. $P < 0.05$ were considered to represent statistically significant differences.

RESULTS

Apoptosis of Chang liver cells by FFAs

We studied the effect of PA, the most abundant saturated fatty acid in vivo, on the Chang "normal" hepatocyte line. We chose Chang cells because they represent a more physiological system as nonmalignant human hepatocytes compared with hepatoma cells (25). RT-PCR analysis showed that Chang cells expressed markers for hepatocytes such as α-fetoprotein, ALT, phosphoenolpyruvate carboxykinase, albumin, tryptophan 2,3-dioxygenase, cytochrome enzymes (Cyp7A1, Cyp3A4), α-1-antitrypsin, and cytokeratin 8 (**Fig. 2A**) (16). Furthermore, Chang cells cleared 78.8% of added NH_4Cl, which was significantly higher than the clearance by control HeLa cells (8.0%) ($P < 0.05$) (Fig. 2A), suggesting that Chang cells represent authentic hepatocytes. PA induced Chang cell death, as assessed by MTT assay (Fig. 2B). Hoechst/PI staining demonstrated that Chang cell death by PA was a classical apoptosis characterized by nuclear condensation/fragmentation (Fig. 2C). Sub-G1 DNA peak was also observed by DNA ploidy analysis (Fig. 2D). A time course study showed that cell death >50% occurred at 24 h after treatment (Fig. 2E).

Because lipid intermediates produced from PA, such as ceramide, are well-known inducers of apoptosis (26), we investigated whether agents inhibiting the conversion of PA to lipid intermediates could affect Chang cell lipoapoptosis. Triacsin C, which inhibits acyl-CoA synthetase, the first enzyme in the conversion of PA to lipid intermediates through palmityol-CoA (27) (Fig. 1), effectively blocked Chang cell death by PA, suggesting that conversion products of PA but not PA itself induce lipoapoptosis ($P < 0.000005$) (Fig. 2F). We then studied the effect of fumonisin B1, which blocks ceramide synthesis by inhibiting sphingosine *N*-acyltransferase (Fig. 1) (28). Contrary to our expectation, fumonisin B1 did not affect Chang cell death by PA (Fig. 2G). Because this finding was inconsistent with previous reports by others using pancreatic islet cells (4), we next studied the effect of myriocin, which blocks the synthesis of ceramide/sphingosine by inhibiting serine palmitoyltransferase (29) (Fig. 1). Myriocin also did not inhibit Chang cell death by PA (Fig. 2H), suggesting that the conversion of FFAs to lipid intermediates in the sphingolipid-ceramide pathway and finally to ceramide is not involved in the lipoapoptosis of hepatocytes.

We next explored the possible involvement of protein kinase C (PKC) in Chang cell lipoapoptosis, because recent papers showed a role for PKC activation in apoptosis (30) and that PKC activators such as diacylglycerol (DAG) and LPC can be synthesized from palmitoyl-CoA (31) (Fig. 1). Both calphostin C and GF109203X, well-known PKC inhibitors, significantly attenuated Chang cell death by PA, supporting a role for PKC in Chang cell lipoapoptosis ($P < 0.000005$ for both) (see supplementary Fig. I).

Roles of PLA_2 and LPC in lipoapoptosis

We next studied the possible role of PLA_2 in Chang cell lipoapoptosis, because PLA_2 is involved in several cell death models (12, 13) and phosphatidylcholine (PC), a conversion product of DAG, can be a substrate for PLA_2, leading to the production of LPC, another PKC activator (Fig. 1). Intriguingly, aristolochic acid, a general inhibitor of PLA_2, and bromoenol lactone (BEL), a specific inhibitor of $iPLA_2$ (12, 13), markedly inhibited Chang cell death by PA, suggesting important roles for PLA_2 and the conversion products of PA downstream of PLA_2, rather than of DAG upstream of PLA_2, in lipoapoptosis and PKC activation ($P < 0.0001$ and 0.00005, respectively) (**Fig. 3A**). Because these results also suggested the possible involvement of $iPLA_2$ among diverse PLA_2 members, we used other PLA_2 inhibitors that are specific for each type of PLA_2. $PACOCF_3$, another $iPLA_2$-specific inhibitor of a different class (12, 32), dramatically blocked Chang cell death by PA ($P < 0.00005$). MAFP, an inhibitor of cytoplasmic phospholipase A_2 ($cPLA_2$) (12), also significantly blocked Chang cell death by PA ($P < 0.005$). However, the protection by the maximum tolerable MAFP level was less compared with that by $PACOCF_3$ ($P < 0.005$), suggesting that $iPLA_2$ rather than $cPLA_2$ is involved in the lipoapoptosis of hepatocytes (Fig. 3B). Consistent with these pharmacological data, $iPLA_2$ activity was increased significantly after treatment of Chang cells with PA ($P < 0.05$), which was inhibited by BEL ($P < 0.01$) (see supplementary Fig. II).

To confirm the role of $iPLA_2$, we conducted an RNA interference experiment. Transfection of siRNA for $iPLA_2\beta$ or $iPLA_2\gamma$, two major types of $iPLA_2$, significantly attenuated Chang cell death by PA, substantiating the roles of $iPLA_2$ in lipoapoptosis ($P < 0.00005$ for both comparisons) (Fig. 3C). Transfection of $iPLA_2\beta$ and $iPLA_2\gamma$ siRNA markedly decreased the expression of $iPLA_2\beta$ and $iPLA_2\gamma$, respectively, at the RNA level (Fig. 3D). However, the combination of both siRNAs did not induce a further decrease in lipoapoptosis (Fig. 3C).

Next, we studied whether LPC, which is liberated from PC by PLA_2 as the most abundant lysophospholipid in vivo, could indeed be produced from PA. Intracellular LPC content was increased significantly by PA ($P < 0.01$), and the LPC content after PA treatment was attenuated significantly by BEL ($P < 0.05$) (Fig. 3E). In contrast, LPC content in the culture supernatant was not increased after treatment of Chang cells with PA (see supplementary Fig. III). Treatment of Chang cells with exogenous palmitoyl-LPC (~10–50 μM) for 24 h also induced significant cell death in a dose-dependent manner ($P < 0.000001$) (Fig. 3F).

We next tested the effect of pertussis toxin (PTX) on Chang cell lipoapoptosis, because PTX inhibits LPC signaling through G-protein-coupled receptor (GPCR)/$G\alpha_i$ (33, 34). PTX (~100–400 ng/ml) remarkably inhibited Chang cell death by exogenous LPC or PA ($P < 0.00005$ and 0.000000005, respectively) (Fig. 3F). We further studied the role of GPCR/$G\alpha_i$ in lipoapoptosis by transfecting a dominant-negative mutant of $G\alpha_i$ (α_{i2}G203T) (18). Stable Chang cell transfectants expressing α_{i2}G203T were resistant to death by PA or LPC, strongly supporting the role of LPC and GPCR/$G\alpha_i$ in lipoapoptosis of Chang cells (Fig. 3G). Transfection with a control wild-type $G\alpha_{i2}$ did

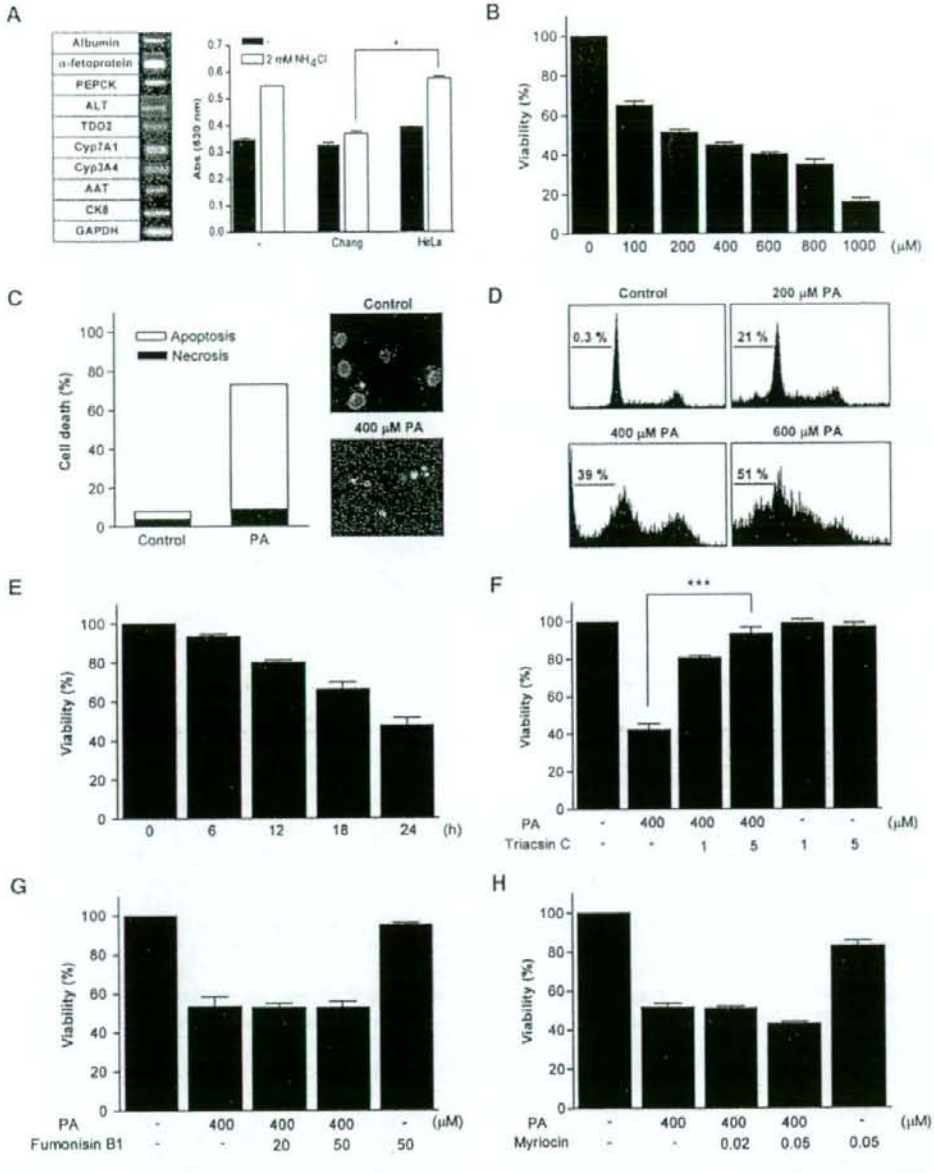

Fig. 2. Apoptosis of Chang liver cells by palmitic acid (PA). A: RT-PCR was conducted using RNA extracted from Chang "normal" liver cells and primers specific for various hepatocyte markers. Removal of exogenous ammonia by Chang cells or control HeLa cells was measured. AAT, α-1-antitrypsin; ALT, alanine aminotransferase; CK8, cytokeratin 8; PEPCK, phosphoenolpyruvate carboxykinase; TDO2, tryptophan 2,3-dioxygenase. B: Chang cells were treated with PA for 24 h, and 3-[4,5-dimethylthiazol-2-yl]-2,5-diphenyltetrazolium bromide (MTT) assay was conducted. C: After the same treatment as in B, Hoechst/propidium iodide (PI) double staining was performed, and the number of cells showing nuclear condensation/fragmentation was counted. D: After the same treatment as in B, DNA ploidy assay was conducted using PI staining followed by flow cytometric analysis. The percentage of cells showing sub-G1 peak was calculated as a measure of nuclear fragmentation. E: Chang cells were treated with PA for the indicated time periods, and MTT assay was performed. More than 50% of the cells died after treatment with 400 μM PA for 24 h. F: After pretreatment with triacsin C, an inhibitor of acyl-CoA synthetase, Chang cells were treated with PA for MTT assay. G, H: After pretreatment with fumonisin B1 or myriocin, inhibitors of ceramide synthesis, Chang cells were treated with PA. Values shown are means ± SD. * $P < 0.05$, *** $P < 0.001$.

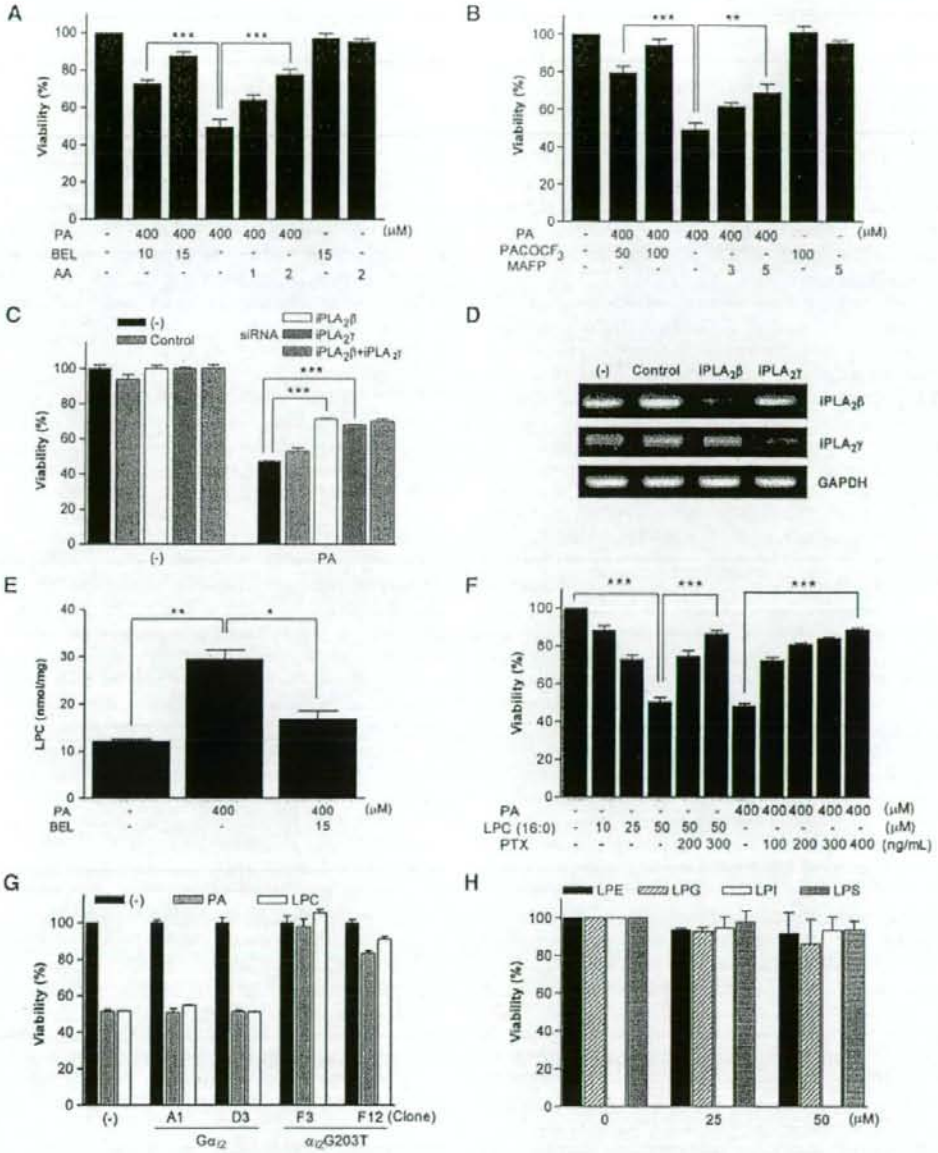

Fig. 3. Role of the PLA_2/LPC pathway in the lipoapoptosis of hepatocytes. A: After pretreatment with aristolochic acid (AA), a general inhibitor of PLA_2, or BEL, an inhibitor of Ca^{2+}-independent phospholipase A_2 ($iPLA_2$), Chang cells were treated with PA. After 24 h of incubation, MTT assay was done. B: Chang cells were pretreated with $PACOCF_3$, another $iPLA_2$-specific inhibitor, or methyl arachidonyl fluorophosphonate (MAFP), a cytoplasmic phospholipase A_2-specific inhibitor, before treatment with PA. The inhibition of lipoapoptosis by MAFP was less pronounced than that with $PACOCF_3$. C: Chang cells were transfected with $iPLA_2\beta$ and/or $iPLA_2\gamma$ small interfering RNA (siRNA) before treatment with PA. An irrelevant siRNA served as a control. D: Expression of $iPLA_2\beta$ and $iPLA_2\gamma$ in siRNA-transfected cells was examined by RT-PCR. E: After PA treatment with or without BEL pretreatment, intracellular LPC content in Chang cells was measured by an enzymatic assay. F: Chang cells were treated with exogenous LPC or PA with or without pertussis toxin (PTX) pretreatment, and cell viability was measured by MTT assay. G: Stable transfectants expressing wild-type $G\alpha_{i2}$ (A1, D3) or a dominant-negative $G\alpha_{i2}$ mutant (F3, F12) were produced by transfection with FuGENE 6 and G418 selection. They were treated with PA or LPC, and MTT assay was done. H: Chang cells were treated with minor products of $iPLA_2$ for 48 h. Values shown are means ± SD. * $P < 0.05$, ** $P < 0.01$, *** $P < 0.001$.

not significantly affect Chang cell death by PA or LPC, probably because of endogenous expression of $G\alpha_i$. We next examined the effect of other lysophospholipids that exist in vivo at much lower concentrations compared with LPC but that could be affected by PLA_2 inhibitors. Lysophosphatidylethanolamine (LPE), lysophosphatidylglycerol (LPG), lysophosphatidylinositol (LPI), or lysophosphatidylserine (LPS) up to 50 μM, which is much higher than their physiological concentrations, induced negligible cell death even at 48 h after treatment, suggesting that the effects of PLA_2 inhibitors are most likely through LPC (Fig. 3H).

We next studied intracellular events associated with lipoapoptosis. We measured the intracellular content of cardiolipin, which is crucial for cytochrome *c* binding to the mitochondrial inner membrane as a mitochondria-specific phospholipid and could be affected by FFA treatment. Cardiolipin content measured by NAO fluorescence began to decrease at ~3–6 h after PA treatment and decreased further at ~12–24 h after treatment (**Fig. 4A**). The PA-induced decrease in cardiolipin content was attenuated significantly by $iPLA_2$ inhibitors such as BEL and $PACOCF_3$, suggesting important roles for PLA_2 or LPC in the decrease of cardiolipin content and lipoapoptosis ($P < 0.0001$ and 0.0005, respectively) (Fig. 4B). We also studied whether LPC could directly induce changes in Bid apart from its receptor-mediated effect, because previous papers reported that Bid could perturb mitochondrial membrane in association with LPC (35). Bid in the mitochondrial fraction was increased by PA treatment, which was inhibited by BEL (Fig. 4C), suggesting a possible role for full-length Bid in cell death by LPC, as reported (35). Probably because of the decrease in cardiolipin content and the increase in Bid in the mitochondria, cytochrome *c* was translocated from mitochondria to cytoplasm and mitochondrial potential was decreased between 3 and 24 h after PA treatment (Fig. 4D). Chang cell death by PA was inhibited significantly by a pancaspase inhibitor, zVAD-fmk, suggesting that effector caspases were activated downstream of cytochrome *c* translocation ($P < 0.000005$) (Fig. 4E). We also studied whether PA activates JNK, because LPC is a well-known activator of JNK (36). Treatment of Chang cells with PA induced JNK activation, which was inhibited by $PACOCF_3$, suggesting that LPC produced from PA is involved in JNK activation (Fig. 4F). Exogenous LPC also induced JNK activation in Chang cells, as expected (Fig. 4F). Stable Chang cell transfectants expressing dominant-negative α_{i2}G203T mutant showed attenuated JNK activation after treatment with PA or LPC, suggesting that LPC produced from PA activates JNK through GPCR/$G\alpha_i$ (Fig. 4G). SP600125 (~10–20 μM), a JNK inhibitor, induced a small but significant decrease in PA-induced death (~25%) ($P < 0.005$), suggesting that JNK activation plays a certain role in the lipoapoptosis of Chang cells (Fig. 4H).

Inhibition of PA-induced lipoapoptosis by oleic acid

Because DAG can be converted to triglyceride (TG) (Fig. 1), we examined the role of TG in lipid injury. PA did not increase intracellular TG content, estimated by Oil Red O staining followed by spectrophotometry or microscopic examination. In contrast, oleic acid (OA), the most abundant unsaturated fatty acid in vivo, markedly increased TG content. Treatment with OA in combination with PA further increased TG content (**Fig. 5A, B**).

Regarding cell viability, OA did not induce Chang cell death. On the contrary, OA significantly blocked Chang cell death by PA ($P < 0.00005$), similar to previous reports (37) (Fig. 5C). OA also abolished the increase in LPC content by PA treatment ($P < 0.00005$) (Fig. 5D), suggesting that increased FFAs lead to either steatosis of hepatocytes attributable to increased TG content or death of hepatocytes attributable to increased LPC content, depending on the absolute/relative abundance of saturated/unsaturated fatty acids (Fig. 1).

Effect of PA on primary hepatocytes

We next used primary hepatocytes instead of cell lines. Hoechst/PI staining showed that PA induced the death of primary human hepatocytes as well, which was a classical apoptosis characterized by nuclear condensation/fragmentation (**Fig. 6A**). Lipoapoptosis of primary human hepatocytes by PA was inhibited by BEL ($P < 0.0005$) but not by fumonisin B1 or myriocin, suggesting that the $iPLA_2$/LPC pathway rather than the ceramide pathway is crucial, similar to Chang cells (Fig. 6B, C). Exogenous LPC also induced the death of primary human hepatocytes, which was inhibited by PTX ($P < 0.0005$) (Fig. 6D). PTX also significantly blocked the death of primary human hepatocytes by PA, suggesting that endogenous LPC induces the death of primary human hepatocytes through GPCR/$G\alpha_i$ ($P < 0.000001$) (Fig. 6D). OA attenuated the death of primary human hepatocytes by PA, supporting our hypothesis that unsaturated fatty acids divert saturated fatty acids into the TG pathway and attenuate primary human hepatocyte death by saturated fatty acids (Fig. 6E). Consistent with the death of primary human hepatocytes, PA induced the release of AST from cultured primary human hepatocytes, which was inhibited by BEL, PTX, or OA. LPC also induced AST release, which was blocked by PTX (Fig. 6F). PA induced the death of primary murine hepatocytes also, as assessed by lactate dehydrogenase release assay. Lipoapoptosis of primary murine hepatocytes by 750 μM PA (33.9 ± 3.8%) was significantly inhibited by 30 μM BEL (26.4 ± 3.6%), 100 μM $PACOCF_3$ (20.5 ± 3.1%), or 300 ng/ml PTX (26.9 ± 1.4%) ($P < 0.05$, 0.01, and 0.05, respectively).

LPC content in NAFLD liver specimens

We next studied whether LPC is able to induce liver injury by directly injecting LPC in vivo. When 60 mg/kg LPC was administered to ICR mice through tail veins, AST/ALT levels were notably increased at 24 h after injection ($P < 0.005$ for both comparisons) (**Fig. 7A**). Hematoxylin and eosin and TUNEL staining of histological sections obtained at 3 days after LPC injection showed lobular hepatitis with a histological score of 1 (focal lytic necrosis, one focus or less per ×100 field) without evidence of steatosis (38) and $TUNEL^+$ apoptotic cells in the

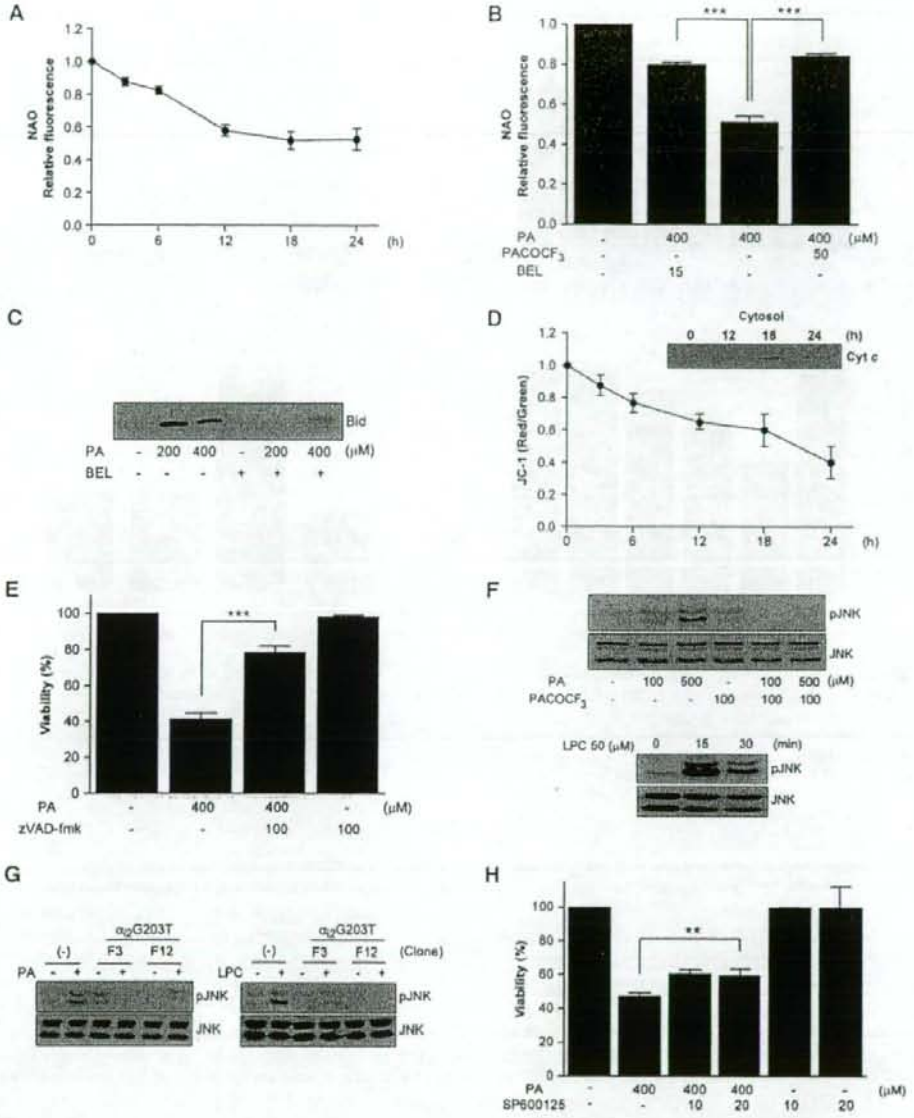

Fig. 4. Intracellular events associated with the lipoapoptosis of hepatocytes. A: Chang cells were treated with PA for the indicated time periods, and 10-*N*-nonyl acridine orange (NAO) fluorescence was determined by flow cytometry as a measure of mitochondrial cardiolipin content. B: Chang cells were treated with PA for 24 h after pretreatment with BEL or $PACOCF_3$, and NAO fluorescence was measured as in A. C: Chang cells were treated with PA with or without BEL pretreatment. After cell fractionation, the presence of Bid in the heavy membrane fraction was examined by Western blotting. D: Chang cells were treated with PA for the indicated time periods and then incubated with JC-1 for 10 min. Emission at 530 and 590 nm was measured, and absorption at 590 nm (A_{590})/A_{530} was calculated as an indicator of mitochondrial potential. Treated cells were fractionated, and the presence of cytochrome *c* in the cytosolic fraction was examined by Western blotting (inset). E: Chang cells were treated with PA after pretreatment with zVAD-fmk, and MTT assay was done. F: Chang cells were treated with PA for 24 h with or without $PACOCF_3$ pretreatment, and cell lysate was subjected to Western blotting using antibodies specific for phosphorylated c-Jun N-terminal kinase (JNK) or total JNK (upper panel). Chang cells were also treated with LPC for the indicated time, and cell lysate was subjected to Western blotting (lower panel). G: Stable transfectants expressing dominant-negative $G\alpha_{12}$ mutant were treated with PA or LPC, and cell lysate was subjected to Western blotting as in F. H: Chang cells were treated with PA after pretreatment with SP600125, a JNK inhibitor, and MTT assay was done. Values shown are means ± SD. ** $P < 0.01$, *** $P < 0.001$.

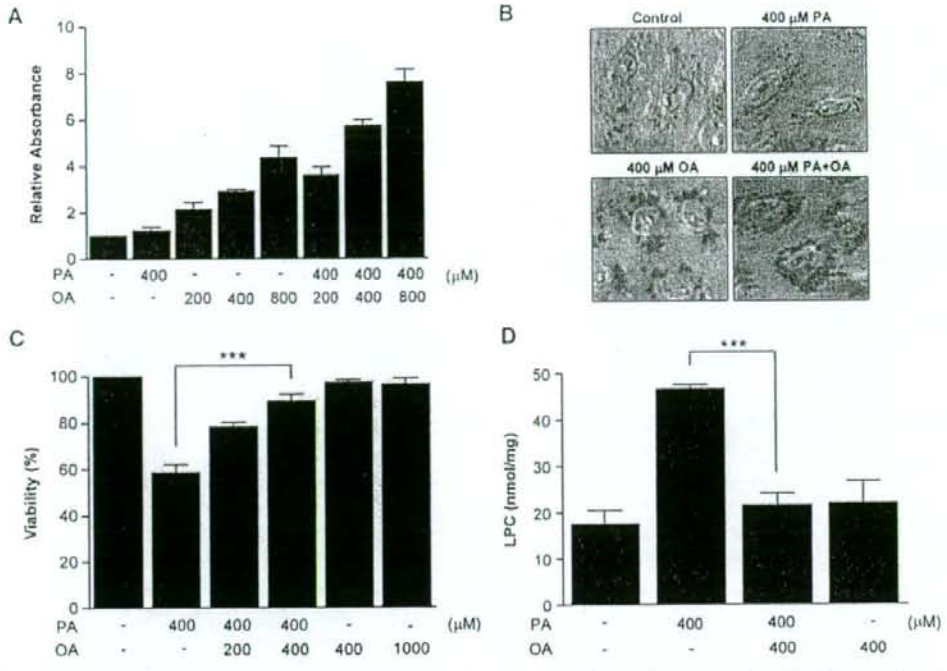

Fig. 5. Effect of unsaturated fatty acids on the lipoapoptosis of hepatocytes. A: Chang cells were treated with various combinations of saturated fatty acid (PA) and unsaturated fatty acid [oleic acid (OA)]. After Oil Red O staining and isopropanol extraction, A_{540} was measured to estimate intracellular TG content. B: After the same treatment and Oil Red O staining as in A, cells were observed with a light microscope. Treatment with OA but not with PA increased intracellular TG content. Combined OA/PA treatment further increased TG content. C: After treatment of Chang cells with various combinations of PA and OA, MTT assay was conducted. D: After the same treatment as in C, intracellular LPC content was measured by an enzymatic assay. Values shown are means ± SD. *** $P < 0.001$.

area of hepatitis, respectively, supporting our hypothesis that LPC plays a role as a mediator of hepatocyte injury in vivo (Fig. 7B).

We finally measured LPC content in liver biopsy specimens. ANOVA revealed that LPC content in the liver specimens from patients with NAFLD was significantly higher than that in the nontumor part of the liver from patients with metastatic colon cancer ($P < 0.005$). LPC content in the liver specimens from patients with NASH (NAFLD class 3–4) appears to be higher compared with that from patients with NAFLD class 2 (lobular hepatitis only); however, the difference was not statistically significant by the Scheffé test ($P > 0.1$) (Fig. 7C).

DISCUSSION

We observed that PA induces the apoptosis of hepatocytes through conversion to LPC, which led to the activation of GPCR, mitochondrial events, and JNK (**Fig. 8**). Although Chang cells and primary hepatocytes from mice or human all underwent apoptosis after treatment with PA, the susceptibility to lipoapoptosis was different, which could be attributable to differences in cell types, species, or the method of cell death assay. Although the identity of Chang cells has been questioned, recent papers have demonstrated the hepatocyte nature of Chang cells based on the expression of α-fetoprotein and albumin (39, 40), which was again supported by our results showing the expression of various markers for hepatocytes and the removal of ammonia by Chang cells. In contrast to our expectation, the conversion of PA to ceramide/sphingosine did not play a role in Chang cell lipoapoptosis, because both fumonisin B1 and myriocin inhibiting ceramide synthesis at two different steps did not block Chang cell lipoapoptosis. These results differ from previous findings suggesting essential roles for ceramide in the lipoapoptosis of pancreatic islet cells or hematopoietic cells (4, 41). However, papers reporting the ceramide-independent lipoapoptosis of various types of cells, including hepatocytes, have also been published (5, 7, 42, 43). These discrepancies might be attributable to differences in cell types or experimental conditions.

Instead of the ceramide pathway, conversion to DAG, PC, and then LPC appears to play an important role in Chang cell lipoapoptosis. Palmitoyl-CoA can be incorpo-

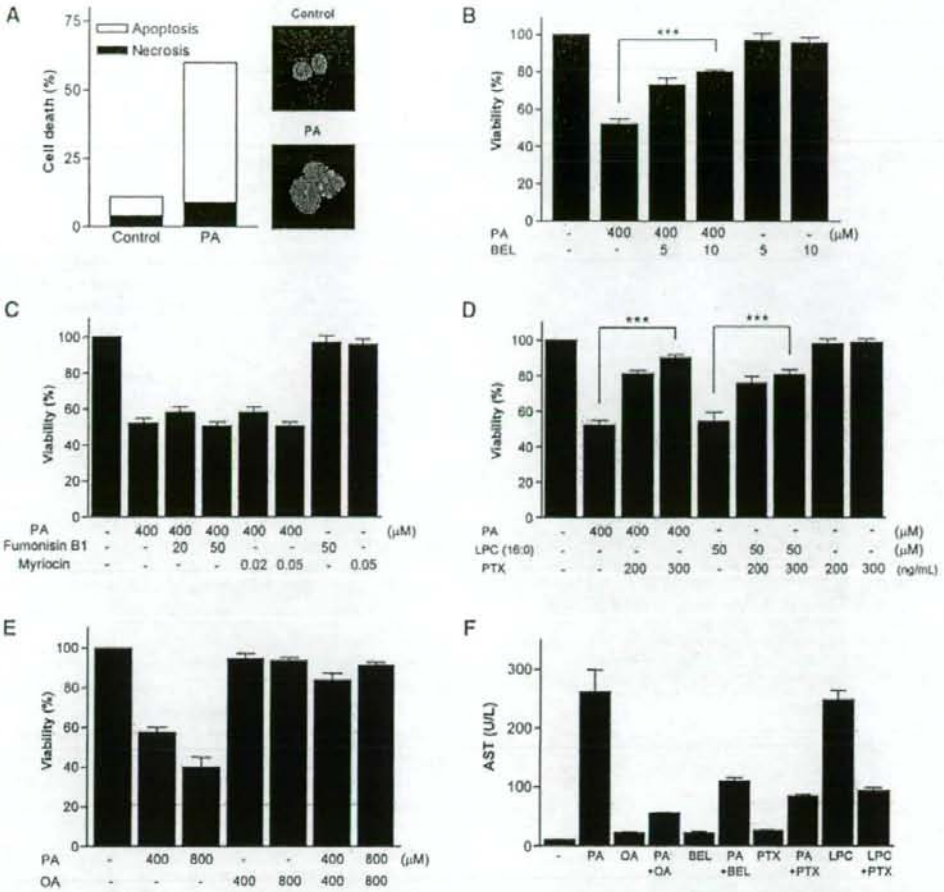

Fig. 6. Death of primary hepatocytes by PA. A: Primary human hepatocytes isolated by two-step collagenase perfusion were treated with PA for 24 h, and Hoechst/PI staining was conducted as in Fig. 2C. B: Primary human hepatocytes pretreated with BEL were incubated with PA as in Fig. 3A, and MTT assay was done. C: Primary human hepatocytes pretreated with fumonisin B1 or myriocin were incubated with PA as in Fig. 2G, H, and MTT assay was conducted. D: After pretreatment with PTX, primary human hepatocytes were treated with PA or exogenous LPC as in Fig. 3F. E: After treatment of primary human hepatocytes with various combinations of PA and OA, MTT assay was conducted as in Fig. 5C. F: After treatment of human primary hepatocytes with PA in the presence or absence of BEL, PTX, or OA, aspartate aminotransferase (AST) level in the supernatant was measured using a blood chemistry analyzer. Values shown are means ± SD. *** $P < 0.001$.

rated to phosphatidic acid, which can be converted to DAG, a well-known PKC activator (30) (Fig. 1). Downstream of DAG, we noticed that DAG could be converted to PC and then to LPC, another PKC activator, by PLA_2 (44). Because PLA_2 participates in several cell death models (12, 13), we investigated whether PLA_2 is involved in the lipoapoptosis of hepatocytes. Our results showing a remarkable inhibition of Chang cell lipoapoptosis by BEL or $PACOCF_3$ suggest the involvement of $iPLA_2$ and LPC rather than DAG upstream of PLA_2. Although BEL has been reported to inhibit phosphatidic acid phosphohydrolase in addition to $iPLA_2$ (24), our finding that another $iPLA_2$-specific inhibitor, $PACOCF_3$, which is structurally unrelated to BEL (24), dramatically inhibited Chang cell death by PA suggests that $iPLA_2$ plays a critical role in lipoapoptosis. Moreover, LPC content was increased significantly after PA treatment of Chang cells and reverted to a normal level with BEL, suggesting an important role of LPC as a death effector in PA-induced lipoapoptosis. However, it is not clear which among several types of $iPLA_2$ that could be inhibited by BEL (45, 46) is responsible for the lipoapoptosis of hepatocytes. Because we observed significant decreases in Chang cell lipoapoptosis with both $iPLA_2\beta$ and $iPLA_2\gamma$ siRNA, a single type of $iPLA_2$ may not

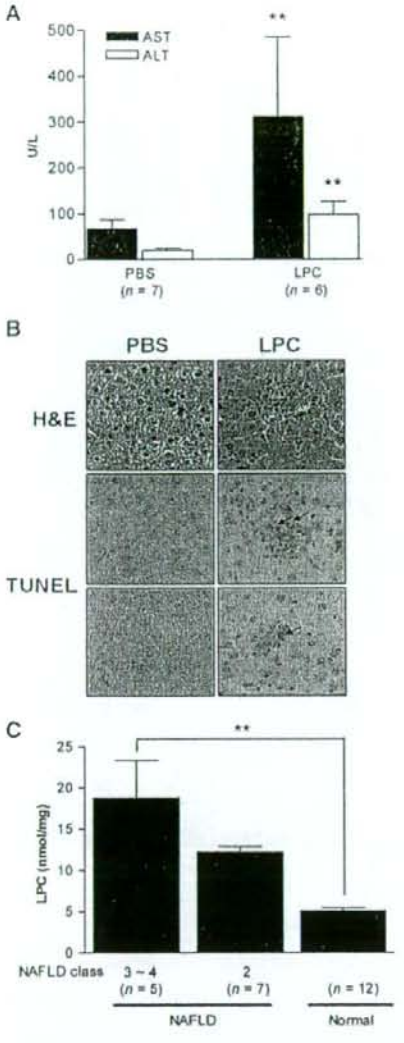

Fig. 7. LPC, liver injury in vivo, and nonalcoholic fatty liver disease (NAFLD). A: LPC was administered into the tail vein of ICR mice, and AST/ALT levels were measured. B: Histological grading of the liver injury was assessed according to a published criteria (38). TUNEL staining was done on the adjacent sections to identify apoptotic hepatocytes in the area of hepatitis. H&E, hematoxylin and eosin. Magnification ×100. C: LPC content was measured in liver biopsy specimens from patients with NAFLD and in the nontumoral part of the liver from patients undergoing hepatic resection for metastatic colon cancer (Normal). The severity of NAFLD was assessed according to a published classification (2). Values shown are means ± SD. ** $P < 0.01$.

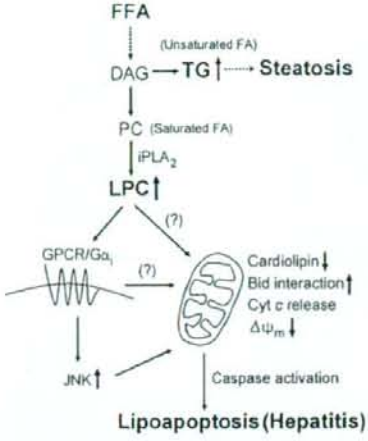

Fig. 8. Proposed model for NAFLD. DAG produced by the incorporation of FFA into the glycerol backbone may be converted to LPC or TG depending on the absolute/relative abundance of saturated/unsaturated fatty acids. Steatosis or hepatitis may occur when the TG pathway or the LPC pathway, respectively, prevails. LPC may induce apoptosis through the activation of G-protein-coupled receptor (GPCR/$G\alpha_i$), mitochondrial events, and JNK.

be fully responsible for the production of LPC from FFAs. Further work will be necessary to elucidate the roles of specific $iPLA_2$ types in lipoapoptosis.

The role of PLA_2 in cell death/survival has been reported in diverse models of hypoxia, reperfusion injury, and reactive oxygen species damage (12, 13, 47, 48). Our results are similar to previous findings showing a significant role of $iPLA_2$ in hypoxic cell injury (12, 47); however, our findings are different from those results in that LPC appears to be an effector downstream of $iPLA_2$ activation. Our data that $iPLA_2$ activity was significantly (nearly 2-fold) increased by PA and that the increased activity was completely reversed by BEL are also similar to previous data that $iPLA_2$ activity was increased in the course of hypoxic cell death (12). The mechanism of the activation of $iPLA_2$ activity by PA is not clearly understood and may involve translocation to target organelles, displacement of inhibitor molecules by FFA-induced endoplasmic reticulum stress, or reactive oxygen species (12, 24, 49). Incomplete protection of PA-induced hepatocyte death by a combination of $iPLA_2\beta$ and $iPLA_2\gamma$ siRNAs or $iPLA_2$ inhibitors such as BEL and $PACOCF_3$ suggests a potential role of $iPLA_2$-independent mechanisms in the lipoapoptosis of hepatocytes. For instance, the role of fatty acid metabolites other than LPC, such as DAG and ceramide, cannot be totally eliminated, because we used mostly pharmacological inhibitors that could have overlapping substrate specificities.

Exogenous LPC has been reported to induce apoptosis (44, 50) and stimulate inflammatory cells (17). However, the proapoptotic role of endogenous LPC has not been reported, to our knowledge. As $iPLA_2$ does not have a

specificity toward PC, the roles of other lysophospholipids cannot be completely eliminated. However, in vivo concentrations of other phospholipids, such as phosphatidylethanolamine, phosphatidylglycerol, phosphatidylinositol, and phosphatidylserine, are around or less than one-tenth of that of PC (51, 52). Much higher in vivo concentrations and much stronger apoptotic activity of LPC compared with LPE, LPG, LPI, or LPS essentially eliminates the possibility that other minor lysophospholipids play significant roles in lipoapoptosis. Previous papers also showed obvious apoptotic activity of LPC, whereas that of other lysophospholipids has not been clearly demonstrated (44, 50). Products of PLA_2 released from PC together with LPC, such as arachidonic acid or its derivatives (10, 11), have diverse effects in vivo. Whereas dipalmitoyl-phosphatidic acid is predominantly produced by PA treatment (53), a certain amount of arachidonic acid may be produced by repeated deacylation and reacylation at the *sn*-2 position and may contribute the phenotypes associated with FFA excess. However, a recent paper showed much weaker activation of stress molecules such as JNK by a variety of unsaturated FFAs, including arachidonic acid, compared with saturated FFAs (54), consistent with our results suggesting that saturated FFAs exert much stronger cytotoxicity compared with unsaturated FFAs.

Intracellular events associated with LPC-induced apoptosis are not clearly defined. Recent papers reported that GPCRs mediate various actions of LPC (33, 34), but it remains controversial whether GPCRs are LPC receptors or mediate LPC actions indirectly. The inhibition of PA- or LPC-induced Chang cell apoptosis by PTX or a dominant-negative $G\alpha_i$ mutant (18) suggests that certain GPCR/$G\alpha_i$ is involved in apoptosis by endogenous or exogenous LPC (55). The effect of a dominant-negative $G\alpha_i$ mutant observed in this study is not mediated by lysophosphatidic acid (LPA), which could be produced from LPC by autotaxin (56), because Chang cell death by PA or LPC was not inhibited by Ki16425, an LPA_1/LPA_3 receptor antagonist (56), and LPA up to 50 μM did not induce Chang cell death (M. S. Han et al., unpublished data). Furthermore, LPA is a well-known survival or growth factor and has been shown to protect cells from apoptosis (57).

Because GPCRs recognize extracellular ligands, LPC might be released to the extracellular space and bind to GPCRs (58). Instead, LPC might enter the receptor binding site in a lateral manner between transmembrane regions of the receptor without leaving the membrane (59), which is more consistent with the absence of the increase of LPC content in the culture supernatant after PA treatment. However, it is not proven whether such a model proposed for LPA is valid for LPC binding to its receptors. Downstream of receptor binding, we observed decreased cardiolipin content after PA treatment, consistent with a previous report (53). The PA-induced decrease in cardiolipin content could be attributable to the inhibition of CDP-DAG synthase, the rate-limiting step in cardiolipin biosynthesis, by LPC, as suggested previously (60). Although a different mechanism, such as poor substrate availability of dipalmitoyl-phosphatidic acid for CDP-DAG synthase, has been proposed (53), the inhibition of lipoapoptosis and the reversal of the decrease in cardiolipin content by PLA_2 inhibitors downstream of phosphatidic acid support a role for LPC rather than dipalmitoyl-phosphatidic acid upstream of PLA_2. The loss of cardiolipin, a mitochondria-specific phospholipid that maintains mitochondrial membrane stability by binding to cytochrome *c* (61), is probably responsible for cytochrome *c* translocation, the loss of mitochondrial potential, and cell death after PA treatment. Besides receptor binding, LPC might directly induce mitochondrial events by recruiting Bid, a well-known initiator of apoptosis, to the mitochondrial membrane (35). JNK activation by saturated FFAs may also contribute to the cytochrome *c* release and lipoapoptosis in hepatocytes, whereas the contribution of JNK activation in the lipoapoptosis of Chang cells does not appear to be dominant. Although we focused on the mitochondrial events associated with LPC accumulation in the course of hepatocyte death by PA, previous papers showed the involvement of other organelles, such as endoplasmic reticulum and lysosome, in the lipoapoptosis of hepatocytes (5–8). Further work will be required to address the potential relationship between the $iPLA_2$/LPC pathway and endoplasmic reticulum stress or lysosomal permeabilization (7, 8, 24).

The inability of OA to induce lipoapoptosis is consistent with JNK activation by saturated FFAs but not by unsaturated fatty acids (54). The increased TG content by OA but not by PA and the further increase by combined OA/PA treatment suggest that an increased channeling of PA into TG plays a protective role against PA-induced lipoapoptosis. Although channeling into TG protects against lipotoxicity, excessive TG may impose deleterious effects on cellular function, such as impaired insulin production in pancreatic β-cells. An increased TG content in the liver leads to steatosis, which is one of the two main features of NAFLD. The preferential increase of TG content by unsaturated fatty acids might be attributable to the increased stability of lipid droplets containing a higher percentage of unsaturated acyl chains (37).

The death of hepatocytes constitutes another main feature of NAFLD, leading to inflammation, fibrosis, and ultimately cirrhosis (NASH). Cells may enter the steatosis track if the DAG→TG pathway prevails or the death track if the DAG→PC→LPC pathway predominates, which might depend on the amount and types of available FFAs or the "second hit," such as inflammatory cytokines (62, 63), that may determine the conversion of steatosis to hepatitis (Fig. 8). Consistent with our in vitro models, we observed increased LPC content in patients with NAFLD depending on the severity of the disease, yet we cannot completely eliminate the possibility that the difference in the methods of tissue sampling between NAFLD tissue and control tissue might have affected the results. The development of hepatitis and increased liver enzymes after LPC administration also provides another line of in vivo evidence supporting the role of LPC in liver injury.

Our results demonstrate that FFAs lead to steatosis or lipoapoptosis according to the absolute/relative abundance of FFAs, consistent with previous epidemiological data reporting more prevalent NASH in patients with a high intake of saturated fatty acids (64). Our data suggest the potential therapeutic values of the modulation of dietary fatty acids and inhibitors of PLA_2 and GPCR/$G\alpha_i$ in the prevention/treatment of hepatocyte injury in NASH. However, caution is advised for PLA_2 and GPCR/$G\alpha_i$ inhibitors as therapeutic agents, because they could have diverse biological effects on various tissues.

This work was supported by the Nano/Bio Science Program (Grant 2004-00716) and 21C Frontier Functional Proteomics Project from the Korean Ministry of Science and Technology (Grant FPR05C1-160). M-S.L. is an awardee of Science Research Center Grant R01-2005-000-10326-0 from the Korea Science and Engineering Foundation. The authors are grateful to J. B. Kim at Seoul National University for helpful discussions. The authors thank S-D. Rhee and H-G. Cheon at Korea Research Institute of Chemical Technology for their kind provision of mice.

REFERENCES

1. Mulhall, B. P., J. P. Ong, and Z. M. Younossi. 2002. Non-alcoholic fatty liver disease: an overview. *J. Gastroenterol. Hepatol.* **17:** 1136–1143.
2. Matteoni, C. A., Z. M. Younossi, T. Gramlich, N. Boparai, Y. C. Liu, and A. J. McCullough. 1999. Nonalcoholic fatty liver disease: a spectrum of clinical and pathological severity. *Gastroenterology.* **116:** 1413–1419.
3. Schattenberg, J. M., R. Singh, Y. Wang, J. H. Lefkowitch, R. M. Rigoli, P. E. Scherer, and M. Czaja. 2006. JNK1 but not JNK2 promotes the development of steatohepatitis in mice. *Hepatology.* **43:** 163–172.
4. Shimabukuro, M., Y. T. Zhou, M. Levi, and R. H. Unger. 1998. Fatty acid-induced β cell apoptosis: a link between obesity and diabetes. *Proc. Natl. Acad. Sci. USA.* **95:** 2498–2502.
5. Wei, Y., D. Wang, F. Topczewski, and M. J. Pagliassotti. 2006. Saturated fatty acids induce endoplasmic reticulum stress and apoptosis independently of ceramide in liver cells. *Am. J. Physiol. Endocrinol. Metab.* **291:** 275–281.
6. Ji, J., L. Zhang, P. Wang, Y. M. Mu, X. Y. Zhu, Y. Y. Wu, H. Yu, B. Zhang, S. M. Chen, and X. Z. Sun. 2005. Saturated free fatty acid, palmitic acid, induces apoptosis in fetal hepatocytes in culture. *Exp. Toxicol. Pathol.* **56:** 369–376.
7. Feldstein, A. E., N. W. Werneburg, Z. Li, S. F. Bronk, and G. J. Gores. 2006. Bax inhibition protects against free fatty acid-induced lysosomal permeabilization. *Am. J. Physiol. Gastrointest. Liver Physiol.* **290:** 1339–1346.
8. Feldstein, A. E., N. W. Werneburg, A. Canbay, M. E. Guicciardi, S. F. Bronk, R. Rydzewski, L. J. Burgart, and G. J. Gores. 2004. Free fatty acids promote hepatic lipotoxicity by stimulating TNF-alpha expression via a lysosomal pathway. *Hepatology.* **40:** 185–194.
9. Malhi, H., S. F. Bronk, N. W. Werneburg, and G. J. Gores. 2006. Free fatty acids induce JNK-dependent hepatocyte lipoapoptosis. *J. Biol. Chem.* **281:** 12093–12101.
10. Schmid, P. C., E. Deli, and H. H. Schmid. 1995. Generation and remodeling of phospholipid molecular species in rat hepatocytes. *Arch. Biochem. Biophys.* **319:** 168–176.
11. Schmid, P. C., I. Spimrova, and H. H. Schmid. 1995. Incorporation of exogenous fatty acids into molecular species of rat hepatocyte phosphatidylcholine. *Arch. Biochem. Biophys.* **322:** 306–312.
12. Shinzawa, K., and Y. Tsujimoto. 2003. PLA_2 activity is required for nuclear shrinkage in caspase-independent cell death. *J. Cell Biol.* **163:** 1219–1230.
13. Cauwels, A., B. Janssen, A. Waeytens, C. Cuvelier, and P. Brouckaert. 2003. Caspase inhibition causes hyperacute tumor necrosis factor-induced shock via oxidative stress and phospholipase A_2. *Nat. Immunol.* **4:** 387–393.
14. Cnop, M., J. C. Hannaert, A. Hoorens, D. L. Eizirik, and D. G. Pipeleers. 2001. Inverse relationship between cytotoxicity of free fatty acids in pancreatic islet cells and cellular triglyceride accumulation. *Diabetes.* **50:** 1771–1777.
15. Suk, K., S. Kim, Y-H. Kim, K-A. Kim, I. Chang, H. Yagita, M. Shong, and M-S. Lee. 2001. IFNγ/TNFα synergism as the final effector in autoimmune diabetes: a key role for STAT1/IRF-1 in pancreatic β-cell death. *J. Immunol.* **166:** 4481–4489.
16. Cai, J., Y. Zhao, Y. Liu, F. Ye, Z. Song, H. Qin, S. Meng, Y. Chen, R. Zhou, X. Song, et al. 2007. Directed differentiation of human embryonic stem cells into functional hepatic cells. *Hepatology.* **45:** 1229–1239.
17. Yan, J. J., J. S. Jung, J. E. Lee, J. Lee, S. O. Huh, H. S. Kim, K. C. Jung, J. Y. Cho, J. S. Nam, H. W. Suh, et al. 2004. Therapeutic effects of lysophosphatidylcholine in experimental sepsis. *Nat. Med.* **10:** 161–167.
18. Winitz, S., S. K. Gupta, N-X. Qian, L. E. Heasley, R. A. Nemenoff, and G. L. Johnson. 1994. Expression of a mutant $Gi_3\alpha$ subunit inhibits ATP and thrombin stimulation of cytoplasmic phospholipase A_2-mediated arachidonic acid release independent of Ca^{2+} and mitogen-activated protein kinase regulation. *J. Biol. Chem.* **269:** 1889–1895.
19. Polyak, K., Y. Xia, J. L. Zweier, K. W. Kinzler, and B. Vogelstein. 1997. A model for p53-induced apoptosis. *Nature.* **389:** 300–305.
20. Chang, I., N. Cho, S. Kim, J. Y. Kim, E. Kim, J-E. Woo, J. H. Nam, S. J. Kim, and M-S. Lee. 2004. Role of calcium in pancreatic islet cell death by IFNγ/TNFα. *J. Immunol.* **172:** 7008–7014.
21. Lee, K. W., J. B. Park, J. J. Yoon, J. H. Lee, S. Y. Kim, H. J. Jung, S. K. Lee, S. J. Kim, H. H. Lee, D. S. Lee, et al. 2004. The viability and function of cryopreserved hepatocyte spheroids with different cryopreservation solutions. *Transplant. Proc.* **36:** 2462–2463.
22. Tong, J. Z., O. Bernard, and F. Alvarez. 1990. Long-term culture of rat liver cell spheroids in hormonally defined media. *Exp. Cell Res.* **189:** 87–92.
23. Nakagawa, T., S. Shimizu, T. Watanabe, O. Yamaguchi, K. Otsu, H. Yamagata, H. Inohara, T. Kubo, and Y. Tsujimoto. 2005. Cyclophilin D-dependent mitochondrial permeability transition regulates some necrotic but not apoptotic cell death. *Nature.* **434:** 652–658.
24. Smani, T., S. I. Zakharov, P. Csutora, E. Leno, E. S. Trepakova, and V. M. Bolotina. 2004. A novel mechanism for the store-operated calcium influx pathway. *Nat. Cell Biol.* **6:** 113–120.
25. Joshi, S. S., C. A. Kuszynski, M. Bakchi, and D. Bagchi. 2000. Chemopreventive effects of grape seed proanthocyanidin extract of Chang liver cells. *Toxicology.* **155:** 83–90.
26. Obeid, L. M., C. M. Linardic, L. A. Karolak, and Y. A. Hannun. 1993. Programmed cell death induced by ceramide. *Science.* **259:** 1769–1771.
27. Knoll, L. J., O. F. Schall, I. Suzuki, G. W. Gokel, and J. I. Gordon. 1995. Comparison of the reactivity of tetradecanoic acids, a triacsin, and unsaturated oximes with four purified *Saccharomyces cerevisiae* fatty acid activation proteins. *J. Biol. Chem.* **270:** 20090–20097.
28. Tonnetti, L., M. C. Veri, E. Bonvini, and L. D'Adamio. 1999. A role for neutral sphingomyelinase-mediated ceramide production in T cell receptor-induced apoptosis and mitogen-activated protein kinase-mediated signal transduction. *J. Exp. Med.* **189:** 1581–1589.
29. Ogretmen, B., B. J. Pettus, M. J. Rossi, R. Wood, J. Usta, Z. Szulc, A. Bielawska, L. M. Obeid, and Y. A. Hannun. 2002. Biochemical mechanisms of the generation of endogenous long chain ceramide in response to exogenous short chain ceramide in the A549 human lung adenocarcinoma cell line. *J. Biol. Chem.* **277:** 12960–12969.
30. Eitel, K., H. Staiger, J. Rieger, H. Mischak, H. Brandhorst, M. D. Brendel, R. G. Bretzel, H. U. Haring, and M. Kellerer. 2003. Protein kinase C delta activation and translocation to the nucleus are required for fatty acid-induced apoptosis of insulin-secreting cells. *Diabetes.* **52:** 991–997.
31. Finney, R. E., E. Nudelman, T. White, S. Bursten, P. Klein, L. L. Leer, N. Wang, D. Waggoner, J. W. Singler, and R. A. Lewis. 2000. Pharmacological inhibition of phosphatidylcholine biosynthesis is associated with induction of phosphatidylinositol accumulation and cytolysis of neoplastic lines. *Cancer Res.* **60:** 5204–5213.
32. Balsinde, J., and E. A. Dennis. 1996. Bromoenol lactone inhibits magnesium-dependent phosphatidate phosphohydrolase and blocks triacylglycerol biosynthesis in mouse P388D1 macrophages. *J. Biol. Chem.* **271:** 31937–31941.
33. Kabarowski, J. H. S., K. Zhu, L. Q. Le, O. N. Witte, and Y. Xu. 2001.

Lysophosphatidylcholine as a ligand for the immunoregulatory receptor G2A. *Science.* **293:** 702–705.
34. Zhu, K., L. B. Baudhuin, G. Hong, F. S. Williams, K. L. Cristina, J. H. S. Kabarowski, O. N. Witte, and Y. Xu. 2001. Sphingosylphosphorylcholine and lysophosphatidylcholine are ligands for the G protein-coupled receptor GPR4. *J. Biol. Chem.* **276:** 41325–41335.
35. Goonesinghe, A., E. S. Mundy, M. Smith, R. Khosravi-Far, J. C. Martinou, and M. D. Esposti. 2005. Pro-apoptotic Bid induces membrane perturbation by inserting selected lysolipids into the bilayer. *Biochem. J.* **387:** 109–118.
36. Fang, X., S. Gibson, M. Flowers, T. Furui, R. C. Bast, and G. B. Mills. 1997. Lysophosphatidylcholine stimulates activator protein 1 and the c-Jun N-terminal kinase activity. *J. Biol. Chem.* **272:** 13688–13689.
37. Listenberger, L. L., X. Han, S. E. Lewis, S. Cases, R. V. Farese, D. S. Ory, and J. E. Schaffer. 2003. Triglyceride accumulation protects against fatty acid-induced lipotoxicity. *Proc. Natl. Acad. Sci. USA.* **100:** 3077–3082.
38. Ishak, K., A. Baptista, L. Bianchi, F. Callea, J. D. Groote, F. Gudat, H. Denk, V. Desmet, G. Korb, R. N. M. MacSween, et al. 1995. Histological grading and staging of chronic hepatitis. *J. Hepatol.* **22:** 696–699.
39. Lee, J-S., and S. S. Thorgeirsson. 2002. Functional and genomic implications of global gene expression profiles in cell lines from human hepatocellular cancer. *Hepatology.* **35:** 1134–1143.
40. Fernandez-Martiniz, A., B. Molla, R. Mayoral, L. Boaca, M. Casado, and P. Martin-Sanz. 2006. Cyclo-oxygenase 2 expression impairs serum-withdrawal-induced apoptosis in liver cells. *Biochem. J.* **398:** 371–380.
41. Paumen, M. B., Y. Ishida, M. Muramatsu, M. Yamamoto, and T. Honjo. 1997. Inhibition of carnitine palmitoyltransferase I augments sphingolipid synthesis and palmitate-induced apoptosis. *J. Biol. Chem.* **272:** 3324–3329.
42. Listenberger, L. L., D. S. Ory, and J. E. Shaffer. 2001. Palmitate-induced apoptosis can occur through a ceramide-independent pathway. *J. Biol. Chem.* **276:** 14890–14895.
43. Hardy, S., W. El-Assaad, E. Przybytkowski, E. Joly, M. Prentki, and Y. Langelier. 2003. Saturated fatty acid-induced apoptosis in MDA-MB-231 breast cancer cells. *J. Biol. Chem.* **278:** 31861–31870.
44. Takahashi, M., H. Okazaki, Y. Ogata, K. Takeuchi, U. Ikeda, and K. Shimada. 2002. Lysophosphatidylcholine induces apoptosis in human endothelial cells through a p38-mitogen-activated protein kinase-dependent mechanism. *Atherosclerosis.* **161:** 387–394.
45. Kinsey, G. R., B. S. Cummings, C. S. Beckett, G. Saavedra, W. Zhang, J. McHowat, and R. G. Schnellmann. 2005. Identification and distribution of endoplasmic reticulum iPLA$_2$. *Biochem. Biophys. Res. Commun.* **327:** 287–293.
46. Jenkins, C. M., D. J. Mancuso, W. Yan, H. F. Sims, B. Gibson, and R. W. Gross. 2004. Identification, cloning, expression, and purification of three novel human calcium-independent phospholipase A_2 family members possessing triacylglycerol lipase and acylglycerol transacylase activities. *J. Biol. Chem.* **279:** 48968–48975.
47. Williams, S. D., and R. A. Gottlieb. 2002. Inhibition of mitochondrial calcium-independent phospholipase A_2 (iPLA$_2$) attenuates mitochondrial phospholipid loss and is cardioprotective. *Biochem. J.* **362:** 23–32.
48. Yellaturu, C. R., and G. N. Rao. 2003. A requirement for calcium-independent phospholipase A_2 in thrombin-induced arachidonic acid release and growth in vascular smooth muscle cells. *J. Biol. Chem.* **278:** 43831–43837.
49. Martinez, J., and J. J. Moreno. 2001. Role of Ca^{2+}-independent phospholipase A_2 on arachidonic acid release induced by reactive oxygen species. *Arch. Biochem. Biophys.* **392:** 257–262.
50. Masamune, A., Y. Sakai, A. Satoh, M. Fujita, M. Yoshida, and T. Shimosegawa. 2001. Lysophosphatidylcholine induces apoptosis in AR42J cells. *Pancreas.* **22:** 75–83.
51. Philips, G. B., and J. T. Dodge. 1967. Composition of phospholipids and of phospholipid fatty acids of human plasma. *J. Lipid Res.* **8:** 676–681.
52. Okita, M., D. C. Gaudette, G. B. Mills, and B. J. Holub. 1997. Elevated levels and altered fatty acid composition of plasma lysophosphatidylcholine (lysoPC) in ovarian cancer patients. *Int. J. Cancer.* **71:** 31–34.
53. Ostrander, D. B., G. C. Sparagna, A. A. Amoscato, J. B. McMillin, and W. Dowhan. 2001. Decreased cardiolipin synthesis corresponds with cytochrome c release in palmitate-induced cardiomyocyte apoptosis. *J. Biol. Chem.* **276:** 38061–38067.
54. Solinas, G., W. Naugler, F. Galimi, M-S. Lee, and M. Karin. 2006. Saturated fatty acids inhibit induction of insulin gene transcription via JNK-mediated phosphorylation of insulin receptor substrates. *Proc. Natl. Acad. Sci. USA.* **103:** 16454–16459.
55. Lin, P., and R. D. Ye. 2003. The lysophospholipid receptor G2A activates a specific combination of G proteins and promotes apoptosis. *J. Biol. Chem.* **278:** 14379–14386.
56. Hama, K., J. Aoki, M. Fukaya, Y. Kishi, T. Sakai, R. Suzuki, H. Ohta, T. Yamori, M. Watanabe, J. Chun, et al. 2004. Lysophosphatidic acid and autotaxin stimulate cell motility of neoplastic and non-neoplastic cells through LPA1. *J. Biol. Chem.* **279:** 17634–17639.
57. Umezu-Goto, M., Y. Kishi, A. Taira, K. Hama, N. Dohmae, K. Takio, T. Yamori, G. B. Mills, K. Inoue, J. Aoki, et al. 2002. Autotaxin has lysophospholipase D activity leading to tumor cell growth and motility by lysophosphatidic acid production. *J. Cell Biol.* **158:** 227–233.
58. van den Besselaar, A. M. H. P., B. de Kruijff, H. van den Bosch, and L. L. M. van Deenen. 1979. Transverse distribution and movement of lysophosphatidylcholine in sarcoplasmic reticulum membranes as determined by ^{13}C-NMR and lysophospholipase. *Biochim. Biophys. Acta.* **555:** 193–199.
59. Xie, Y., T. C. Gibbs, and K. E. Meier. 2002. Lysophosphatidic acid as an autocrine and paracrine mediator. *Biochim. Biophys. Acta.* **1582:** 270–281.
60. Xu, F. Y., W. A. Taylor, and G. M. Match. 1998. Lysophosphatidylcholine inhibits cardiolipin biosynthesis in H9c2 cardiac myoblast cells. *Arch. Biochem. Biophys.* **349:** 341–348.
61. Ott, M., J. D. Robertson, V. Gogvadze, B. Zhivotovsky, and S. Orrenius. 2002. Cytochrome *c* release from mitochondria proceeds by a two-step process. *Proc. Natl. Acad. Sci. USA.* **99:** 1259–1263.
62. Ryden, M., E. Arvidsson, L. Blomqvist, L. Perbeck, A. Dicker, and P. Arner. 2004. Targets for TNF-α-induced lipolysis in human adipocytes. *Biochem. Biophys. Res. Commun.* **318:** 168–175.
63. Yang, S. Q., H. Z. Lin, M. D. Lane, M. Clemens, and A. M. Diehl. 1997. Obesity increases sensitivity to endotoxin liver injury: implications for the pathogenesis of steatohepatitis. *Proc. Natl. Acad. Sci. USA.* **94:** 2557–2562.
64. Musso, G., R. Gambino, F. De Michieli, M. Cassader, M. Rizzetto, M. Durazzo, E. Faga, B. Silli, and G. Pagano. 2003. Dietary habits and their relations to insulin resistance and postprandial lipemia in nonalcoholic steatohepatitis. *Hepatology.* **37:** 909–916.

Am J Physiol Endocrinol Metab 295: E1349–E1357, 2008.
First published October 7, 2008; doi:10.1152/ajpendo.90704.2008.

Bis deficiency results in early lethality with metabolic deterioration and involution of spleen and thymus

Dong-Ye Youn,[1]* Dong-Hyoung Lee,[1]* Mi-Hyun Lim,[1] Jung-Sook Yoon,[2] Ji Hee Lim,[2] Seung Eun Jung,[1] Chung Eun Yeum,[3] Cheol Whee Park,[2] Ho-Joong Youn,[2] Jae-Seon Lee,[4] Seong-Beom Lee,[3] Masahito Ikawa,[5] Masaru Okabe,[5] Yoshihide Tsujimoto,[6,7] and Jeong-Hwa Lee[1]

[1]*Department of Biochemistry,* [2]*Department of Internal Medicine, and* [3]*Department of Pathology, College of Medicine, Catholic University of Korea and* [4]*Division of Radiation Cancer Research, Korea Institute of Radiological and Medical Science, Seoul, Korea; and* [5]*Genome Information Research Center, Research Institute for Microbial Diseases, Osaka University,* [6]*Department of Medical Genetics, Laboratory of Molecular Genetics, Osaka University Medical School, and* [7]*Solution-Oriented Research for Science and Technology, Japan Science and Technology Agency, Osaka, Japan*

Submitted 18 August 2008; accepted in final form 25 September 2008

Youn DY, Lee DH, Lim MH, Yoon JS, Lim JH, Jung SE, Yeum CE, Park CW, Youn HJ, Lee JS, Lee SB, Ikawa M, Okabe M, Tsujimoto Y, Lee JH. Bis deficiency results in early lethality with metabolic deterioration and involution of spleen and thymus. *Am J Physiol Endocrinol Metab* 295: E1349–E1357, 2008. First published October 7, 2008; doi:10.1152/ajpendo.90704.2008.— Bcl-2 interacting cell death suppressor (Bis), also known as Bag3 or CAIR-1, is involved in antistress and antiapoptotic pathways. In addition to Bcl-2, Bis binds to several proteins, suggesting it has diverse functions in normal and pathological conditions. To better define the physiological function of Bis in vivo, we developed *bis*-deficient mice with a *cre-loxP* system. Targeted disruption of exon 4 of the *bis* gene was demonstrated by Southern blotting and PCR, and Western blotting showed that no intact or truncated Bis protein was synthesized in $bis^{-/-}$ mice. While heterozygotes were fertile and appeared normal, Bis-deficient mice showed growth retardation and died by 3 wk after birth. The relative weight of the thymus and spleen was reduced and the total numbers of white blood cells, splenocytes, and thymocytes were significantly reduced compared with wild-type littermates. Serum profiles indicated significant hypoglycemia as well as decrease in triglyceride and cholesterol levels. Expression profiles of metabolic genes indicated that gluconeogenesis and β-oxidation are activated in the liver of $bis^{-/-}$ mice. This activation, as well as a decrease in peripheral fat and an induction of fatty liver, appears to be an adaptive response to hypoglycemia. Our study reveals that the absence of Bis has considerable influences on postnatal growth and survival, possibly due to a nutritional impairment.

bis; knockout; hypoglycemia

THE BCL-2 INTERACTING DEATH SUPPRESSOR (*bis*) gene has been identified as encoding a Bcl-2 binding protein in protein interaction techniques (18). Bis has also been reported as Bag3 and CAIR-1, which bind to heat shock protein (HSP)70 and PLC-γ, respectively (7, 33). The ability of Bis to bind to several proteins suggests that it has distinct functions depending on its cellular environment. A possible role for Bis in modulating cell death was revealed in in vitro DNA transfection experiments in which Bis was shown to significantly enhance the antiapoptotic function of Bcl-2 (18). Supporting this, Bis has also been shown to be specifically expressed or overexpressed in several cancers, including pancreatic cancer, thyroid carcinoma, and some leukemia (1, 5, 21, 27, 28). Furthermore, the downmodulation of Bis results in an increased susceptibility for the induction of apoptosis in cancer cells (1, 5, 26). Bis has been also proposed as an antistress protein, based on the upregulation of its expression, concomitant with HSP70, in cells exposed to stressful stimuli such as heat shock or heavy metals (21, 23). In addition to the stressful conditions given for cellular levels, the expression of Bis is significantly upregulated in several in vivo disease models such as stroke and seizure models (19, 20, 31). Moreover, Bis is robustly expressed in reactive astrocytes in areas of gliosis in the brain of human immunodeficiency virus (HIV) encephalopathy patients (29). Light damage also increases the expression of Bis in the mouse retina (4). These results suggest that the expression of Bis may be induced to protect cells from stressful conditions, but the persistent and/or uncontrolled expression of Bis may contribute to the progression of cancer.

In addition to its possible role as a stress- or survival-related protein, Bis has been implicated to have other cellular functions. Overexpression of Bis promotes the differentiation of human promyelocytic cells and cell cycle arrest (32). Roles for Bis in cell adhesion and migration have been recently reported by separate groups, although their results differ: in one study overexpression of Bis is shown to inhibit the migration and adhesion of breast cancer cell lines, whereas in the other study *bis*-deficient fibroblasts have reduced motility and delayed formation of focal adhesion complex (12, 14). These results suggest that complex mechanisms are involved in the regulation of cellular motility by Bis. Furthermore, cytoplasmic Bis protein modulates the transcription of the HIV-1 gene and the replication of the varicella-zoster virus (15, 29). Therefore, it appears that Bis exerts diverse functions in pathophysiological conditions in vivo, which may be partly ascribed to its ability to interact with several known and yet to be identified proteins.

To better define the function of Bis in vivo, we developed *bis*-deficient mice with a *cre-loxP* system targeting exon 4. Here we show that disruption of exon 4 of the *bis* gene by homologous recombination led to a complete inhibition of Bis protein synthesis, which resulted in serious hypoglycemia, a fatty liver, and 100% lethality before 3 wk of age. Bis-deficient mice also exhibited a significant involution of the spleen and thymus. Our results are inconsistent with a previous study in

* D.-Y. Youn and D.-H. Lee contributed equally to this work.
Address for reprint requests and other correspondence: J.-H. Lee, 505 Banpo-Dong, Seocho-gu, Seoul 137-701, Korea (e-mail: leejh@catholic.ac.kr).

The costs of publication of this article were defrayed in part by the payment of page charges. The article must therefore be hereby marked "*advertisement*" in accordance with 18 U.S.C. Section 1734 solely to indicate this fact.

which retrovirus-targeted deletion of the *bis* gene resulted in massive degeneration of myofibrils with apoptotic features in heart and skeletal muscles and no abnormalities in other organs (10). Possible explanations for the differences observed in *bis*-deficient mice in the previously published study and the present study are discussed below.

METHODS

Construction of targeting vector and generation of bis-mutant mice. A 6,018-bp genomic clone that includes coding exons 3 and 4 of the *bis* gene (nucleotides 17173-23356 from the start codon) was cloned from D3 mouse embryonic stem (ES) cells as the long arm and introduced into a pMulti-ND 1.0 vector with *Pme*I and *Pac*I sites (11). The *loxP* sequences were inserted into an *Eco*RV site located between exon 3 and exon 4. For homologous recombination, the downstream short arm spanning nucleotides 23357-27370 was also cloned and introduced into a *Not*I site of a pMulti vector. The resulting *Pme*I-digested targeting vector was electroporated into D3 ES cells derived from 129Sv and screened for neomycin resistance. Of 98 neomycin-resistant clones, four clones were shown to have the desired homologous recombination as determined by Southern blotting with two different probes for the 5′ and 3′ regions external to the targeting vector and one probe for the neomycin sequences. Four homologous recombinant ES clones were independently injected into C57B6 blastocysts to generate chimeric mice. Male chimera derived from one ES clone transmitted the recombinant allele to the next generation. To generate heterozygous mutants with deletion of exon 4 of the *bis* gene on one chromosome, the germ line-transmitted male mice were mated with *CAG-cre* C57B6 females.

All research procedures involving animals were performed in accordance with the Laboratory Animals Welfare Act, the *Guide for the Care and Use of Laboratory Animals*, and the Guidelines and Policies for Rodent Experiments provided by the Institutional Animal Care and Use Committee (IACUC) at the College of Medicine, Catholic University of Korea and were reviewed and approved by the IACUC.

Southern blotting and allele-specific genomic PCR. Genomic DNA extracted from wild-type or *bis*-mutant mice livers was digested with *Bam*HI enzyme and electrophoresed through 0.8% agarose. After transfer onto nylon membrane by capillary blotting, the membrane was hybridized with a digoxigenin (DIG)-labeled specific DNA probe and then immunodetected with alkaline phosphatase-conjugated anti-DIG antibody and a chemiluminescent substrate (Roche Applied Science, Mannheim, Germany) as described previously (17). The following primers were used to incorporate DIG-11 dUTP for the DNA probes: 5′-TGA GGT AAG AAG AGA CCC AGA GAC (forward primer) and 5′-TAC AGA CGT AGG AAA CAC ATC TCC (reverse primer).

PCR reactions were also performed to detect the truncated *bis* allele in genomic DNA with two sets of primers, 5′-TGA GAG CCA GCA TGC TGT TTC ATT and 5′-TGG CCC TCA GGG GAC AAC CTG CAG designed to amplify a region of 500 bp in the wild-type allele and 5′-CTT TCA AGG ATT TAA CTT ATC TGA CCA and 5′-ACA GCA AGC ATA TTC CTC TAC CTA AG to amplify a 3,003-bp product in the wild-type allele and a 1,043-bp product in the post-*cre* allele. PCR products were electrophoresed on a 1.5% agarose gel and visualized with ethidium bromide staining.

Western blotting. Proteins from various tissues of wild-type or *bis*-mutant mice were prepared and Western blotting was performed as described previously (17). To analyze Bis expression, the blotted membranes were incubated with polyclonal antibodies against the COOH-terminal half of human Bis (306-575 aa) (18) or against whole human Bis (Abnova, Taiwan, Taipei). Polyclonal antibodies raised in rabbit against the NH_2-terminal of human Bis (48-63 aa) (Peptron, Daejeon, Korea) were also used to detect smaller truncated Bis proteins. Antibodies for HSP70 and Bcl-2 were purchased from BD Biosciences (San Jose, CA) and Santa Cruz Biotechnology (Santa Cruz, CA), respectively.

Complete blood count and assay of metabolites in blood and liver. The complete blood count was determined with a Hemavet 850 automated hematologic analyzer (CDC Technologies, Oxford, CT). The concentration of glucose in the blood was determined by Hemocue Glucose 201+ (Hemocue, Angelholm, Sweden). Plasma concentration of insulin was measured with a mouse insulin enzyme-linked immunoabsorbent assay kit (Linco Research, Erie, PA). Measurements of triglyceride, free fatty acid, and cholesterol in the serum and in the liver were performed with the Triglyceride E-test, NEFA-HR (2), and Labassay Cholesterol, respectively (Wako Pure Chemical Industries, Osaka, Japan).

Histological analysis. Paraffin sections (10 μm) from various organs were processed for hematoxylin and eosin (H & E) staining. Frozen liver sections (6 μm) were fixed with 10% formalin, stained with 0.5% Oil Red O, and counterstained with Mayer's hematoxylin. To examine the state of apoptosis in situ in muscles, a terminal deoxynucleotidyl transferase-mediated dUTP nick end labeling (TUNEL) assay was also performed with the ApopTag Peroxidase In Situ Apoptosis Detection Kit S7100 (Chemicon, Temecula, CA). Specimens were examined under a light microscope (Axioskop40, Carl Zeiss, Gottingen, Germany). For electron microscopy, the tissue samples were fixed with 2.5% glutaraldehyde for 1 h. After fixation, the samples were postfixed in 1% O_5O_4, dehydrated in ethanol, and embedded in Epon 812 (Polysciences, Warrington, PA). Ultrathin sections were contrasted with uranyl acetate and lead citrate. Sections were examined in a JEM 1010 CX transmission electron microscope (JEOL, Akishima, Japan).

RNA extraction and quantitative real-time PCR. Total RNA from liver was isolated with RNA-Bee (Tel-Test, Friendswood, TX). cDNA was synthesized from 2 μg of total RNA with AccuPower Cycle Script (dN6) (Bioneer, Daejeon, Korea). mRNA levels of genes involved in glucose and lipid metabolism were measured by quantitative real-time PCR using a cDNA template and appropriate primers as previously described (Refs. 9, 25, 34; Supplemental Table S1).[1] Quantitative real-time PCR was performed with the IQ5 Real Time PCR detection System (Bio-Rad Laboratories, Hercules, CA) and iQ TM SYBR Green Supermix (Bio-Rad Laboratories). Relative levels of PCR products were determined after normalizing to an endogenous cyclophilin control.

Statistical analysis. The number of mice in each experimental group is indicated in Figs. 2 and 3. A two-tailed Student's *t*-test was used to calculate *P* values. All values are presented as means ± SE. Differences were considered significant if $P < 0.05$.

RESULTS

Targeting the bis gene and generation of bis-mutant mice. The coding region of mouse *bis* consists of four exons. The 315-amino acid peptide encoded by exon 4 includes the bag domain and a proline-rich region, which are required for the regulation of HSP70 chaperone activity and cellular motility, respectively (14, 33). To disrupt exon 4, we generated a targeting vector in which exon 4 was bracketed by *loxP* sites as shown in Fig. 1*A*. The germ line-transmitted male mice were obtained and mated with *CAG-cre* C57B6 females as described in METHODS. The resulting heterozygous male *bis* mutants were backcrossed into C57B6 females for more than eight generations to minimize the contribution of the 129Sv genetic background of ES cells on the phenotype of *bis* mutants. Male and female *bis* heterozygotes were interbred to generate homozygous mice. In $bis^{-/-}$ mice, the *loxP* sites and the intervening

[1] The online version of this article contains supplemental material.

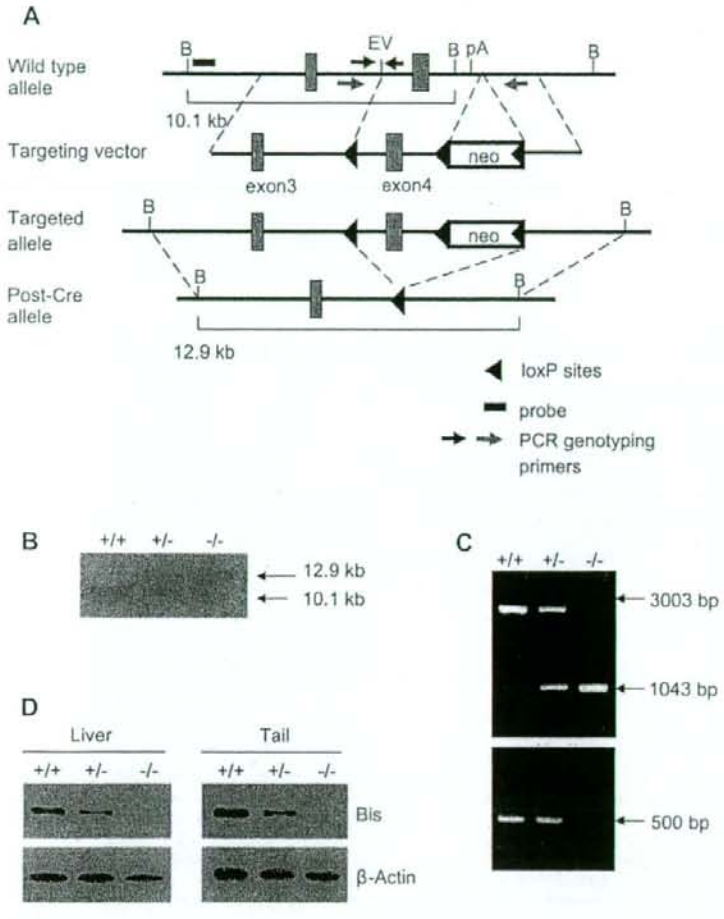

Fig. 1. Targeted disruption of the *bis* gene. *A*: schematic representation of a part of the *bis* genomic locus, targeting vector, and mutant allele. The targeting vector includes the 5′ long arm, the neomycin-resistant gene (*neo*), and the 3′ short arm for homologous recombination. Exon 4, as well as *neo*, was flanked by *loxP* sequences, shown as arrowheads. The sizes of *Bam*HI DNA fragments are indicated beneath the wild-type allele and post-*cre* allele. The 5′ external probe used for Southern blotting is shown as a black square. The small black and gray arrows indicate the locations of the primers used for genotyping. B, *Bam*HI; EV, *Eco*RV; pA, poly A. *B*: Southern blot analysis. Genomic DNA (10 μg) was extracted from liver of mice of the indicated *bis* genotypes. Hybridization of genomic DNA with the external probe, shown in *A*, revealed a 10.1-kb *Bam*HI fragment for wild-type allele and a 12.9-kb *Bam*HI fragment for knockout allele, corresponding to the deletion of a *Bam*HI site and exon 4 by *Cre* excision. *C*: PCR analysis. Genomic DNA was isolated from mouse tails, and PCR screening was performed with 2 pairs of primers, indicated in *A*. A pair of primers (gray arrows in *A*) were designed to produce a 3,003-bp product from the wild-type allele and a 1,043-bp product from the post-*cre* allele. Another pair of primers (black arrows in *A*) failed to amplify a 500-bp product in homozygous $bis^{-/-}$ mice because of the deletion of a section of DNA that contained the reverse primer site. *D*: Western blotting using whole protein extracts from liver and tail revealed that there is no intact Bis protein in $bis^{-/-}$ mice.

DNA, including a *Bam*HI site, were deleted, generating a 12.9-kb fragment of *Bam*HI compared with a 10.1-kb fragment in $bis^{+/+}$ mice, as shown in a Southern blot using genomic DNA extracted from the tail (Fig. 1*B*). PCR analysis using two pairs of primers, upstream and downstream of either the first *loxP* site or all three *loxP* sites, also confirmed the elimination of the DNA fragment flanked by the *loxP* sites (Fig. 1*C*). Expression of the 80-kDa Bis protein was reduced in $bis^{+/-}$ heterozygous and undetectable in $bis^{-/-}$ homozygous mouse liver tissues in a Western blot with Bis-specific antibody against the COOH terminus of Bis (Fig. 1*D*). Neither anti-Bis antibodies raised against whole peptides of Bis nor anti-Bis antibodies specific for its NH_2 terminus showed any smaller size of Bis protein products in heterozygous and homozygous tissues, excluding the possibility of the presence of truncated Bis protein composed of exon 1 from exon 3 (Supplemental Fig. S1). Therefore, disruption of exon 4 of the *bis* gene resulted in the complete inhibition of synthesis of both intact Bis protein and aberrant forms of Bis.

General characteristics of $bis^{-/-}$ mice. The $bis^{-/-}$ offspring were born roughly in a Mendelian ratio: 67 $bis^{-/-}$ homozygous, 135 $bis^{+/-}$ heterozygous, and 75 $bis^{+/+}$ wild type. While $bis^{+/-}$ heterozygous mice appeared normal and were fertile, all $bis^{-/-}$ homozygous mice died before 3 wk of age. As shown in Fig. 2*A*, the difference in body weight between homozygous $bis^{-/-}$ and both heterozygous and wild-type mice was imperceptible at birth but became noticeable within 1 wk after birth and obvious until 12–13 days after birth. Thereafter, the $bis^{-/-}$ mice failed to gain weight and began to gradually lose body weight before they died. Apparently, the thymus and spleen of $bis^{-/-}$ mice shrank dramatically to 51% and 36% of wild type, respectively, in terms of weight per total body weight at 16 days after birth (Fig. 2, *C* and *D*). The involution of spleen in *bis*-deficient mice appeared before that of thymus, showing a reduction of relative weight to 50% of wild type at 14 days after birth but no reduction of thymus (Fig. 2*E*). In addition, the external surface of livers from $bis^{-/-}$ mice, which were 80% of the relative weight of wild-type livers, appeared pale (Fig. 2, *C*

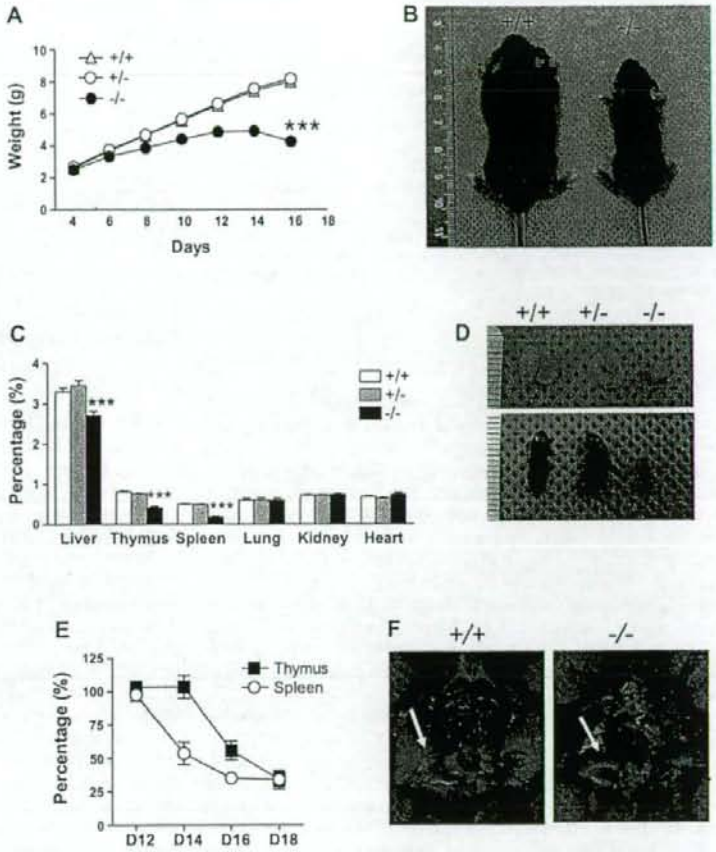

Fig. 2. Characterization of *bis*-deficient mice. *A*: growth of wild-type and $bis^{-/-}$ mice. Offspring generated from heterozygous intercrosses of $bis^{+/-}$ mice were weighed at 2-day intervals from 4 days until 16 days after birth. [n = 46 for wild-type (+/+), 104 for $bis^{+/-}$, 36 for $bis^{-/-}$]. ***$P < 0.001$, compared with wild-type littermates. *B*: representative picture showing significant growth retardation of a $bis^{-/-}$ mouse compared with a wild-type littermate at 16 days of age. *C*: relative weight of each organ to total body weight as shown as %. The ratios of thymus and spleen weight to total body weight in homozygous $bis^{-/-}$ mice were significantly decreased compared with those in wild-type and heterozygous mice older than 16 days of age (n = 15 for $^{+/+}$, 12 for $bis^{+/-}$, 16 for $bis^{-/-}$). ***$P < 0.001$, compared with wild-type littermates. *D*: representative morphology of thymus (*top*) and spleen (*bottom*) at 16 days of age showing notable reduction in size in *bis*-deficient mice. *E*: the decreased size of the thymus and spleen in *bis*-deficient mice was not obvious until age 12 days; thereafter, shrinkage of the spleen occurred before that of the thymus. The relative weight of the thymus and the spleen in $bis^{-/-}$ mice was compared with that of wild-type littermates, and the ratio is shown as %. The data are means ± SE. The number of animals measured each day is 4, 6, 8, and 5 for days (D)12, 14, 16, and 18, respectively. *F*: reduction of subcutaneous fat (white arrow) and periepididymal fat (black arrow) in a male *bis*-deficient mouse at 16 days of age compared with a wild-type male littermate.

and *F*). Notably, the subcutaneous fat and the perigonadal fat were severely reduced in $bis^{-/-}$ mice compared with wild-type mice at day 16 (Fig. 2*F*).

Decreased number of thymocytes, splenocytes, and leukocytes in peripheral blood of bis-deficient mice. As predicted from the reduced size of the thymus and spleen of *bis*-deficient mice, the number of splenocytes and thymocytes was significantly decreased, about one-tenth and one-fifth compared with wild type in the spleen and thymus, respectively, at ≥16 days of age (Table 1). The *bis*-deficient mice also had a >50% decrease in the number of total peripheral leukocytes, but the proportion of neutrophils and lymphocytes was not significantly different from that in wild-type littermates (Table 1). The difference in the number of red blood cells and platelets in *bis*-deficient and wild-type mice was insignificant.

Bis deficiency caused hypoglycemia and hepatic steatosis. The reduction in perigonadal and subcutaneous fat in $bis^{-/-}$ mice suggested that the mice suffered from malnutrition and led us to inspect the metabolic parameters in the serum. As shown in Table 2, serum glucose levels were decreased to one-third the levels of wild type in $bis^{-/-}$ mice. Insulin levels were also lower in *bis*-deficient mice than in $bis^{+/+}$ mice, showing that the hypoglycemia observed in the $bis^{-/-}$ mice was not due to high levels of insulin. Total cholesterol and triglyceride levels were also significantly decreased in *bis*-deficient mice, 60% and 26% of those in wild-type littermates, respectively. The levels of β-hydroxybutyrate, a product of

Table 1. *Comparison of cellularity in spleen and thymus and total blood cell counts in wild-type and bis-deficient mice*

	$bis^{+/+}$	$bis^{-/-}$
Splenocytes, $\times 10^8$	46.2±11.4 (7)	4.67±1.12 (12)*
Thymocytes, $\times 10^7$	16.7±2.79 (7)	2.97±0.87 (12)†
RBC, $\times 10^{12}$/l	6.18±0.18 (9)	6.77±0.16 (13)*
Platelets, $\times 10^9$/l	333±47.2 (9)	329±48.2 (13)
WBC, $\times 10^9$/l	6.63±0.63 (9)	2.76±0.34 (13)‡
Neutrophils	1.72±0.25 (9)	0.71±0.13 (13)†
Lymphocytes	3.98±0.32 (9)	1.63±0.17 (13)‡
Others	0.84±0.18 (9)	0.42±0.07 (13)*

Values are means ± SE for numbers of animals in parentheses. RBC, red blood cells; WBC, white blood cells; Others, monocytes, eosinophils, and basophils. *$P < 0.05$, †$P < 0.01$, ‡$P < 0.001$ compared with $bis^{+/+}$ littermates.

Table 2. *Profile of serum metabolites of wild-type and bis-deficient mice*

Parameter	$bis^{+/+}$	$bis^{-/-}$
Glucose, mg/dl	212.9±11.9 (13)	71.46±4.03 (17)‡
Insulin, pg/ml	768.5±119.7 (7)	282.9±77.5 (11)†
TAG, mg/dl	158.6±21.3 (7)	41.7±11.7 (7)‡
FFA, meq/l	1.2±0.2 (7)	1.0±0.2 (7)
Cholesterol, mg/dl	137.7±11.6 (7)	80.4±5.3 (7)‡
β-Hydroxybutyrate, mmol/l	2.80±0.56 (3)	6.44±1.30 (3)*

Results were obtained from mice at age 16 days and expressed as means ± SE for numbers of animals indicated in parentheses. TAG, triglyceride; FFA, free fatty acids. *$P < 0.05$, †$P < 0.01$, ‡$P < 0.001$ compared with wild-type littermates.

ketogenesis, were increased in $bis^{-/-}$ mice to ~2.5-fold above wild-type levels.

Although no obvious changes were observed by H & E staining (data not shown), Oil Red O staining revealed marked accumulation of lipids throughout the $bis^{-/-}$ liver tissues (Fig. 3*A*). Ultrastructural analysis of the hepatocytes of $bis^{-/-}$ mice revealed the presence of enlarged lipid particles and an increased number of lipid particles (Fig. 3*B*). The lipid contents of the $bis^{-/-}$ livers were analyzed to identify the type of accumulated lipids. In contrast to the serum profile of free fatty acids (FFA), which showed no difference between $bis^{-/-}$ and $bis^{+/+}$ mice, hepatic FFA levels in $bis^{-/-}$ livers were increased to twofold compared with wild-type littermates. $bis^{-/-}$ mice also had 2.8-fold and 3.4-fold increases in hepatic triglyceride and cholesterol levels, respectively, compared with control mice (Fig. 3*C*).

Quantitative RT-PCR revealed increased hepatic expression of mRNAs involved in gluconeogenesis in $bis^{-/-}$ mice, including glucose 6-phosphatase (G6Pase) and phosphoenolpyruvate carboxykinase (PEPCK) (Fig. 3*D*). The expression of several lipogenic genes, including fatty acid synthase (FAS) and stearoyl-CoA desaturase-1 (SCD-1), was markedly diminished, suggesting that de novo synthesis of fatty acids is inhibited in $bis^{-/-}$ mice (Fig. 3*D*). In addition, several hepatic genes involved in β-oxidation, such as carnitine palmitoyltransferase I (CPT-1) and medium-chain acyl-CoA dehydrogenase (MCAD), were induced in $bis^{-/-}$ mice (Fig. 3*D*). Thus hepatic steatosis in $bis^{-/-}$ mice is likely due to fatty acid delivery that exceeds the capacity for hepatic fatty acid oxidation to generate energy for gluconeogenesis, which are the typical metabolic changes in response to fasting (3, 8).

Bis deficiency caused no prominent apoptosis in diaphragm and cardiomyocytes. Bis is highly expressed in skeletal muscles (18), and a previous study with mice in which the *bis* gene had been disrupted by retroviral insertion described that, as the only abnormal finding, *bis*-deficient mice developed a fulminant myopathy characterized by noninflammatory myofibrillar degeneration with apoptotic features (10). However, in our model, no significant differences in H & E staining were found between the skeletal muscles from wild-type and *bis*-deficient mice (Fig. 4*A*), and the ventricular cardiomyocytes revealed similar frequencies in cells positive for TUNEL staining in wild-type and $bis^{-/-}$ mice (Fig. 4*B*). The diaphragm of $bis^{-/-}$ mice revealed a slight increase in TUNEL-positive apoptotic cells (Fig. 4*C*) but not as prominent as previously described by Homma et al. (10). When wild-type mice with body weight similar to $bis^{-/-}$ mice at day 12 after birth were fasted for 48 h, TUNEL-positive cells were increased in the diaphragm compared with feeding control (data not shown). Thus the increase of apoptotic cells in the diaphragm of $bis^{-/-}$ mice might represent a nutritionally insufficient status rather than acceleration of apoptosis due to the absence of Bis. Although no considerable abnormalities were noted in H & E staining, ultrastructures of muscles from *bis*-deficient mice exhibited discontinuous arrangement of myofibrils with thick and short Z bands but nuclei preserved normal morphology (Fig. 4*D*). Previous reports showed the colocalization of Bis with Z-disk proteins such as α-actinin and desmin (10). Thus Bis protein may contribute to preservation of the architecture of myofibrils, especially the integrity of Z bands, rather than the viability of myocytes.

DISCUSSION

Bis is expressed in various tissues, including skeletal muscle, heart, and kidney, and known to bind with several proteins, suggesting that it has diverse physiological functions. Using a *cre-loxP* system, we generated *bis* knockout mice and showed that these mice died within 3 wk after birth with metabolic derangements such as hypoglycemia and hepatic steatosis and significant reduction in the cellularity of the thymus and spleen. A previous study with mice in which the *bis* gene had been disrupted by retroviral insertion also reported premature death before weaning, although these mice died ~1 wk later than the time of death we observed (10). Furthermore, the previous study described severe degeneration and apoptosis in skeletal muscles and myocardium and no evidence of abnormality in other organs (10). In the present study, we found that the skeletal muscle fibers from $bis^{-/-}$ mice were irregular and smaller than those of wild-type littermates but found no evidence for massive apoptosis in the diaphragm, quadriceps, and cardiac muscles (Fig. 4 and data not shown). In addition, several of the phenotypes we report here, such as shrinkage of lymphoid organs and perturbations in metabolic homeostasis, were not observed in the previous report.

At present, the precise reasons for the differences in the phenotypes of our model and the previous model are not entirely clear. The method used for gene targeting may contribute to the different phenotypes observed. The previous *bis*-deficient model was developed with ES clones that had been mutagenized by retroviral insertion (10); our *bis*-deficient mice model was developed by precise deletion of exon 4 of the *bis* gene with a *Cre-loxP* system. Although the previous report does not describe which part of the *bis* gene was disrupted by retroviral insertion, partial disruption of the *bis* gene may have resulted in the expression of truncated Bis protein products, and these may have retained some function. In our system, we did not detect any full-length or truncated Bis protein by Western blotting using three kinds of antibodies raised against whole, COOH-terminal, and NH_2-terminal Bis peptides (Fig. 1 and Supplemental Fig. S1). However, the possibility that the sensitivity of immunoblotting was not high enough to detect a tiny amount of truncated Bis protein in our assay, as well as in the previous model, cannot be excluded. Another possible explanation for the discrepancy in the reported phenotypes of *bis*-deficient mice may be the extent of homogeneity in the genetic background. Diverse genetic backgrounds in hybrid